

Free oxide ion abundances in Na, Ba, and K silicate glasses from O 1s XPS, ^{29}Si NMR, Raman, and MD simulations

G. Michael Bancroft, H. Wayne Nesbitt, John S. Tse, Grant S. Henderson, and Ben J. A. Moulton

Citation: Chin. Phys. B, 2026, 35 (**5**): 056102. DOI: 10.1088/1674-1056/ae3606
http://cpb.iphy.ac.cn; http://iopscience.iop.org/cpb

What follows is a list of articles you may be interested in

Physical properties of Cr_2S_3 at high pressure

Lun Xiong(熊伦), Mingquan Jiang(江明全), Jinxia Zhu(竹锦霞), Lin Xia(夏林), Hao Wang(王毫), Shenghan Zhang(张升瀚), Pengfei Tang(汤鹏飞), Zhiqiang Chen(陈志强), Sheng Jiang(蒋升), and Hongliang Dong(董洪亮)
Chin. Phys. B, 2026, 35 (**3**): 036103. DOI: 10.1088/1674-1056/ae1cb3

Elasticity of quasi-bcc ammonia hemihydrate at high pressures

Mengqiong Pu(蒲梦琼), Jiacheng Zhang(张家诚), Xinyang Li(李新阳), Xiaomei Yuan(苑晓美), Xue Zhang(张雪), Shuo Gao(高硕), Chenlu Wang(王晨璐), Liang Li(李亮), Fangfei Li(李芳菲), and Qiang Zhou(周强)
Chin. Phys. B, 2026, 35 (**3**): 036101. DOI: 10.1088/1674-1056/ae330a

Pressure-induced amorphization and metallization in orthorhombic SiP

Qiru Zeng(曾琪茹), Youjun Zhang(张友君), Yukai Zhuang(庄毓凯), Linfei Yang(杨林飞), Qiming Wang(王齐明), and Yi Sun(孙熠)
Chin. Phys. B, 2025, 34 (**9**): 096102. DOI: 10.1088/1674-1056/add4f6

Layer-dependent structural stability and electronic properties of $CrPS_4$ under high pressure

Jian Zhu(朱健), Dengman Feng(冯登满), Liangyu Wang(王亮予), Liang Li(李亮), Fangfei Li(李芳菲), Qiang Zhou(周强), and Yalan Yan(闫雅兰)
Chin. Phys. B, 2025, 34 (**6**): 066102. DOI: 10.1088/1674-1056/adc65f

Enhanced electronic and photoelectrical properties of two-dimensional Zn-doped SnS_2

Xichen Chuai(揣喜臣), Peng Yin(殷鹏), Jiawei Wang(王嘉玮), Guanhua Yang(杨冠华), Congyan Lu(陆丛研), Di Geng(耿玓), Ling Li(李泠), Can Liu(刘灿), Zhongming Wei(魏钟鸣), and Nianduan Lu(卢年端)
Chin. Phys. B, 2025, 34 (**5**): 056101. DOI: 10.1088/1674-1056/adbaca

---

SPECIAL TOPIC — John Tse: Pioneer in high-pressure materials science

Free oxide ion abundances in Na, Ba, and K silicate glasses from O 1s XPS, ^{29}Si NMR, Raman, and MD simulations

G. Michael Bancroft[1,†], H. Wayne Nesbitt[2], John S. Tse[3], Grant S. Henderson[4], and Ben J. A. Moulton[5]

[1] *Department of Chemistry, University of Western Ontario, London, ON N6A 5B7 Canada*
[2] *Department of Earth Sciences, University of Western Ontario, London, ON N6A 5B7 Canada*
[3] *Department of Physics and Engineering Physics, University of Saskatchewan, Saskatoon, SASK S7N 5E2 Canada*
[4] *Department of Earth Sciences, University of Toronto, Toronto, ON M5S 3B1 Canada*
[5] *Inamori School of Engineering, New York College of Ceramics, Alfred University, Alfred, New York* 14802 *USA*

(Received 23 October 2025; revised manuscript received 6 January 2026; accepted manuscript online 9 January 2026)

In alkali silicate glasses with $\leq$ 50 mol% M_2O (M = Na, K, Rb, Cs), the existence of $>$ 1 mol% reactive "free" oxide (FO, where O is not bonded to Si) has been a highly controversial topic over the past 15 years. Unlike their crystalline analogues, Raman and ^{29}Si nuclear magnetic resonance (NMR) studies since 1980 have shown that two or more Q^n (n =0–4) species are present in silicate glasses over a wide range of compositions. For example, M_2SiO_3 crystals contain only Q^2 species; however, glasses of the same composition exhibit Q^1 and Q^3 in addition to Q^2. Previous Raman and NMR studies on alkali silicate glasses have related the abundances of these three species solely through disproportionation reactions (e.g. $2Q^2 \Leftrightarrow Q^1 + Q^3$). In doing so, polymerization reactions (e.g. $2Q^2 \Leftrightarrow 2Q^3 + \mathrm{FO}$) were completely neglected. By combining published O 1s x-ray photoelectron spectroscopy (XPS) spectra, ^{29}Si NMR and Raman results for 40 mol% and 50 mol% Na_2O, K_2O, and BaO glasses, together with new molecular dynamics (MD) simulations of Na_4SiO_4 glass, we provide consistent and compelling evidence for the existence of $>$ 1 mol% FO in these glasses and melts. In particular, for 50 mol% K_2O silicate glass, all three experimental techniques estimate FO to be $\geq$ 7 mol%, while MD simulations of Na_4SiO_4 yield $\sim$ 5 mol% FO. Our analysis requires revised assignments (challenging decades of "conventional wisdom") for ^{29}Si NMR and Raman spectra, based on O mass balance, recognition of M–BO bonding effects first identified in O 1s XPS spectra, and quantitative analysis of Raman spectra for 40–50 mol% Na_2O, K_2O, and BaO glasses. These FO values are comparable to those now accepted for alkaline-earth silicate glasses. The importance of this reactive FO for chemical reactivity (e.g. with H_2O and CO_2), bioactivity, and physical properties (e.g. melting) of silicate glasses is discussed.

Keywords: alkali silicate glasses, free oxide (Na–O–Na), O 1s XPS, Raman, ^{29}Si NMR

PACS: 61.43.Fs, 79.60.–i, 76.60.–k, 78.30.–j

DOI: 10.1088/1674-1056/ae3606 **CSTR:** 32038.14.CPB.ae3606

1. Introduction

In contrast to the well-established atomic-level crystal structures of stoichiometric crystalline alkali and alkaline-earth silicates (e.g. $Na_2Si_2O_5$,[1] Na_2SiO_3,[2] $MgSiO_3$,[3] and Mg_2SiO_4[4]), the atomic-level structures of silicate glasses with similar compositions remain insufficiently characterized, even after $\sim$ 90 years since the pioneering x-ray diffraction studies of silicate glasses by Zachariasen[5] and Warren and Briscoe.[6,7] By combining these early x-ray studies with more recent Na and Si x-ray absorption fine structure (XAFS),[8,9] neutron diffraction,[10] and molecular dynamics (MD) simulations,[11–15] the Si–O and Na–O bond lengths, as well as the O–Si–O and O–Na–O bond angle distributions, are now well established.

Despite the fundamental importance of SiO_4 tetrahedra in both glasses and minerals, glasses are much more complex than their crystalline counterparts (see Refs. [16–18] for reviews). First, glasses lack long-range order, and the nature of Na–O bonding in the traditionally accepted modified random network (MRN) model,[18,19] including subsequent modifications for Na–BO bonding,[20,21] remains poorly understood in detail (even after numerous MD simulations).[11–15] Second, in contrast to crystalline silicates, which exhibit only a limited number of discrete compositions (e.g. disilicates, metasilicates, and orthosilicates such as $Na_2Si_2O_5$, Na_2SiO_3, and Mg_2SiO_4, respectively), glasses (and melts) span a wide compositional range. Indeed, silicate glasses can be regarded as solid solutions of M_2O (e.g. Na_2O) or MO (e.g. MgO) with SiO_2, with compositions ranging from $<$ 1 mol% MO to $>$ 66.7 mol% MO. This compositional range can be rationalized using the depolymerization equation[22]

$$x\mathrm{Na_2O} + (1-x)\mathrm{SiO_2} \Leftrightarrow (\mathrm{Na_2O})_x(\mathrm{SiO_2})_{1-x}, \quad (1)$$

or

$$\mathrm{O^{2-}} + \mathrm{BO} \Leftrightarrow 2\mathrm{NBO^-}, \quad (2)$$

†Corresponding author. E-mail: gmbancro@uwo.ca

© 2026 Chinese Physical Society and IOP Publishing Ltd. All rights, including for text and data mining, AI training, and similar technologies, are reserved.

where O^{2-} represents the oxide ion or free oxygen (FO, an oxygen not bonded to Si, also known as non-network oxygen), BO denotes bridging oxygen (O in the Si–O–Si moiety), and NBO^- denotes non-bridging oxygen (O in the Si–O–M moiety). The equilibrium constant for reaction (2) is

$$K_3 = \frac{[\mathrm{NBO}]^2}{[\mathrm{FO}]\cdot[\mathrm{BO}]}. \tag{3}$$

Clearly, if FO = 0, then $K_3 = \infty$, and each Na_2O unit provides one O^{2-} that attacks a BO (Si–O–Si), producing 2NBO (Na–O–Si); however, if K_3 is finite, some FO (e.g. Na–O–Na) must remain. This simple yet critical thermodynamic equilibrium implies that some FO should exist at all Na_2O concentrations in these solid solutions, even if it may not be experimentally detectable at low Na_2O contents. Third, unlike minerals such as $Na_2Si_2O_5$ and Na_2SiO_3, which contain only Q^3 [$Si(BO)_3(NBO)$] and Q^2 [$Si(BO)_2(NBO)_2$] species, respectively (where the superscript in Q^n denotes the number of BO units), significant progress was made in the 1970s and 1980s using Raman spectroscopy[23–28] and ^{29}Si magic angle spinning (MAS) nuclear magnetic resonance (NMR)[29–32] to demonstrate the presence of additional Q^n species (for example, Q^2 and Q^4, in addition to Q^3, in $Na_2Si_2O_5$ glass). For instance, Raman spectra of sodium silicate glasses from 1975–1984[23–28] showed peaks corresponding to Q^1, Q^2, and Q^3 at ~ 850 cm^{-1}, ~ 950 cm^{-1}, and ~ 1100 cm^{-1}, respectively, assigned to the A_1 symmetric stretching modes of these structural units. Shortly thereafter, ^{29}Si NMR studies of Na silicate glasses[29–32] identified Q^2 and Q^3 peaks at ~ 77 ppm and ~ 88 ppm. These findings highlighted the opportunity to quantify the distribution of Q species in alkali and alkaline-earth silicate glasses. Such distributions, together with the quantification of NBO, BO, and FO, are critical for understanding the chemical and physical properties of melts. For example, Fine and Stolper[33,34] sought to identify the reactive species responsible for converting H_2O to OH and CO_2 to CO_3^{2-}, and noted the potential importance of FO in these reactions. However, subsequent interpretations within the NMR and Raman communities largely dismissed the presence of FO, leading to the assumption that NBO is the reactive species. Later, we reinterpreted Stolper's data and proposed that FO is, in fact, the reactive species.[35]

How are these multiple Q species related? Can equilibrium constants such as K_3 in Eq. (3) be calculated for the entire Na_2O–SiO_2 solid solution? How large is [FO] in these glasses? Answering these questions using O 1s XPS and Raman spectra has been a major goal of our research since 2007 and is the focus of this paper. In the literature prior to 1970 (before the observation of distinct Q species by ^{29}Si NMR or Raman spectroscopy[23–32] or the resolution of BO and NBO in early O 1s XPS[36,37]), several studies[38–40] proposed polymerization of SiO_4 units in melts, which is a potential mechanism for conversion between Q species

$$2Q^0 \Leftrightarrow 2Q^1 + \mathrm{FO}. \tag{4}$$

Other similar polymerization reactions are possible (for $n = 1,2,3$)

$$2Q^n \Leftrightarrow 2Q^{n+1} + \mathrm{FO}. \tag{5}$$

Given these earlier studies, it is perhaps surprising that early Raman[23–28] and NMR researchers[29–32] in the 1980s related the Q species exclusively through disproportionation reactions

$$2Q^n \Leftrightarrow Q^{n-1} + Q^{n+1}, \tag{6}$$

for example

$$2Q^3 \Leftrightarrow Q^2 + Q^4, \tag{7a}$$

or

$$2Q^2 \Leftrightarrow Q^1 + Q^3. \tag{7b}$$

In the 1980s, Schramm *et al.*[29] mentioned the possibility of FO in Li silicate glasses, and Maekawa *et al.*[41] in 1991 showed evidence of FO in Li silicates from ^{29}Si NMR. Neither study, however, linked FO explicitly to the polymerization reactions in Eqs. (4) and (5). Despite the higher resolution of Raman spectra compared to ^{29}Si NMR, Raman data could not be reliably assigned or quantified.[23–28] In contrast, the high-quality resolved ^{29}Si NMR spectrum of a 41 mol% Na_2O glass enriched in ^{29}Si could be quantified, and Stebbins[32] obtained the first equilibrium constant K (0.011 ± 0.005) for reaction (7a) from the integrated areas of the Q^2 and Q^3 peaks in the ^{29}Si MAS NMR spectrum, combined with the Q^4 contribution from a static ^{29}Si spectrum. Only the disproportionation framework was used to relate the three Q species. Ironically, as discussed below, this work[32] is the first to indicate the presence of a few mol% FO (and the importance of polymerization reactions) in an alkali or alkaline-earth silicate glass. As an aside, the disproportionation reaction (Eqs. (6) and (7)) does not change the number of Si–O–Si bonds or the NBO/Si ratio in a glass or melt, regardless of the reaction extent (e.g. Eq. (2) for Na_2SiO_3 and Eq. (4) for Na_4SiO_4).

^{29}Si (and ^{17}O) NMR[41–48] and Raman[49–59] studies on alkali and alkaline-earth silicate glasses over the following four decades relied entirely on disproportionation reactions, with no consideration of possible polymerization reactions. A consensus and "conventional wisdom" emerging from "group thinking"[60] held that disproportionation was the only relevant mechanism linking Q species, and therefore FO was so small that it could be neglected. As stated in several reviews on FO in Na and K silicate glasses by Stebbins and coworkers,[61–63] any significant FO "seems to be highly unlikely".[62] In 2020, Stebbins[63] further concluded from

new ^{29}Si and ^{17}O NMR studies of ~ 50 mol% Na_2O and K_2O glasses that any FO in Na or K glasses was below detection limits of approximately 0.5%–1.0% FO.

When we attempted to publish results on Na silicates using a different technique (O 1s XPS) in 2011,[64] more than 25 years after many of the above NMR and Raman studies, the manuscript was rejected–rejection of the technique, rejection of the results, and rejection of the interpretation. The paper was ultimately published approximately 18 months after initial submission, following three rounds of revision, inclusion of new ^{29}Si NMR spectra, and constructive editorial support that encouraged open discussion. This outcome was surprising, given that our first O 1s XPS study on Pb silicates in 2007[65] demonstrated that high-resolution XPS optimized for non-conducting samples under ultra-clean conditions yields well-resolved and readily interpretable O 1s spectra, in good agreement with ^{29}Si NMR results,[66] and reveals substantial FO (19.5 mol% at 66.7 mol% PbO), corresponding to $K_3 \sim 12$. This work initiated a broader discussion on FO in Na and K silicates following our XPS study of K silicate glasses,[35] along with Malfait's response[67] and our rebuttal.[68] Subsequent studies by Stebbins[61–63] acknowledged FO in Pb, Ca, and Mg silicates after our 2015 work[69] and additional NMR and Raman studies of alkaline-earth silicates near the orthosilicate composition, which reported several mol% FO.[70–73] However, those studies[61–63] continued to reject significant FO in Na and K glasses. The prevailing "conventional wisdom" therefore maintained that FO is negligible in Na and K silicates. Indeed, even recent Raman and ^{29}Si NMR studies on alkali silicate glasses[74–78] continue to interpret the data solely in terms of disproportionation reactions.

Five years after Stebbins' last rebuttal,[63] it is timely to present our perspective, supported by both new results and a reanalysis of previously published data. We have not been able to publish further papers on the FO controversy in Na and K silicates since our 2015 contributions[35,68,69] noted above. However, over the past decade, we have shown that Raman spectra can be reliably assigned and quantified;[79–83] these assignments have been independently confirmed in several recent Raman studies.[77,84–86] Some of these studies have carefully considered the role of FO in Na and Ba silicate glasses.[83–85] For example, we have shown that 40 and 50 mol% Na_2O glasses contain measurable amounts of FO based on both Raman and ^{29}Si NMR spectra,[81,83] in agreement with earlier O 1s XPS results.[64] Notably, the FO content we obtain for the 40 mol% Na_2O glass is identical to that calculated from the data in Stebbins' 1987 study.[32]

Perhaps the most compelling recent evidence for significant FO in K silicate glasses comes from newly published Raman spectra of 33–50 mol% K silicate glasses,[76] which enable direct comparison with earlier ^{29}Si NMR spectra.[41,46,63] Reanalysis of these data yields substantial FO contents from the ^{29}Si NMR spectra, consistent with FO values obtained from earlier O 1s XPS measurements.[35,68,87] In addition, our new MD simulations of Na_4SiO_4 glass show appreciable concentrations of Si–O–Si dimers and FO arising from polymerization reactions such as Eq. (5).

The main objective of this paper is to provide conclusive evidence for mol% FO in alkali silicate glasses using O 1s XPS, a reanalysis of published ^{29}Si NMR and Raman spectra, and new MD simulations. To achieve this objective, we first evaluate the strengths and limitations of the three spectroscopic techniques. We show that O 1s XPS, when performed under stringent ultra-high-vacuum conditions, is a reliable method for determining the molar fractions of BO, NBO, and FO in Pb, Na, and K glasses. For Pb silicate glasses, the large FO values obtained from O 1s XPS over a wide compositional range are confirmed by ^{29}Si and ^{17}O NMR,[66,88] whereas the NMR community has argued against the validity of the XPS-derived FO values for Na and K silicates, based on poorly resolved NMR spectra.[61–63] Second, we summarize our efforts to resolve the long-standing challenge of assigning and quantifying Raman spectra of silicate glasses,[18,83–85,89] showing that quantitative determination of Q^1, Q^2, and Q^3 species in 40–50 mol% alkali glasses is now achievable in many cases. Third, using our revised ^{29}Si NMR and Raman assignments for 40 mol% Na_2O and 40 mol% BaO glasses,[83–85] we demonstrate that the only consistent interpretation of recent Raman spectra of 50 mol% K_2O samples contradicts previous NMR-based assignments[41,67,68] that assumed the absence of FO. In short, the ^{29}Si NMR spectra of 50 mol% K_2O glass have been misassigned since 1991,[41,46,63] and the FO content is substantial ($\geq$ 7 mol%) in this composition, consistent with XPS results.[35,68] Fourth, we present new MD simulations of Na_4SiO_4 glass, which reveal significant populations of Q^1 dimers from reaction (4), along with FO. Fifth, we highlight several oversights and post hoc adjustments made within the ^{29}Si and ^{17}O NMR and Raman literature after the community consensus formed that FO does not exist in alkali silicate glasses, a viewpoint that likely led Maekawa[41] to misassign his ^{29}Si NMR spectrum of the 50 mol% K_2O glass despite an initially more straightforward interpretation. Finally, we hope that this work also contributes to a broader discussion on the nature and application of the scientific method in the Earth sciences, as elegantly discussed by Richet.[60]

1.1. The critical importance of spectral resolution

As discussed above, three unrelated spectroscopic techniques — NMR (^{29}Si and ^{17}O), Raman spectroscopy, and O 1s XPS — have been used to estimate the abundances of Q^n species (n = 0–4) and O species (BO, NBO, and FO) in alkali and alkaline-earth silicate glasses. Spectral resolution is

a critical property in any spectroscopic analysis. Without sufficient peak resolution, it is not possible to obtain reliable or objective estimates of Q species or of NBO, BO, and FO populations. As noted above, the resolved ^{29}Si NMR spectrum of a 41 mol% Na_2O glass yielded the first quantitative equilibrium constant K_3 for relating Q^2, Q^3, and Q^4 (Eq. (7a)).[32,42] However, ^{29}Si NMR spectra are generally less well resolved than Raman spectra of the same glass compositions. The most important and influential of these NMR spectra is that of the 50 mol% Na_2O glass shown in Fig. 1.[41] There is broad agreement on the assignment of the three features in this spectrum: a weak, narrow Q^1 peak at 67 ppm, an intense Q^2 peak at 76 ppm, and a broad, poorly resolved Q^3 contribution at approximately 80–84 ppm. The question remains whether the Q^1 and Q^3 species can be reliably quantified from such a partially resolved spectrum. We emphasize again that, from Eq. (7b), $Q^3 = Q^1$ for pure disproportionation; whereas $Q^3 \gg Q^1$ if polymerization reactions also occur, implying the presence of FO.

The 1987/1991 spectra recorded at relatively low magnetic fields (e.g. 4.7 T by Maekawa,[41] shown here in Fig. 11(a)) are, in practice, as well resolved as spectra obtained by us at 9.4 T in 2011,[64] or those measured at 14 T by Stebbins in 2020.[63] Moreover, the 1991 spectrum is the best available for accurate digitization. It exhibits good signal-to-noise ratio, and the experimental points are reported individually rather than as smoothed curves. Consequently, the 1991 spectrum is the best available.

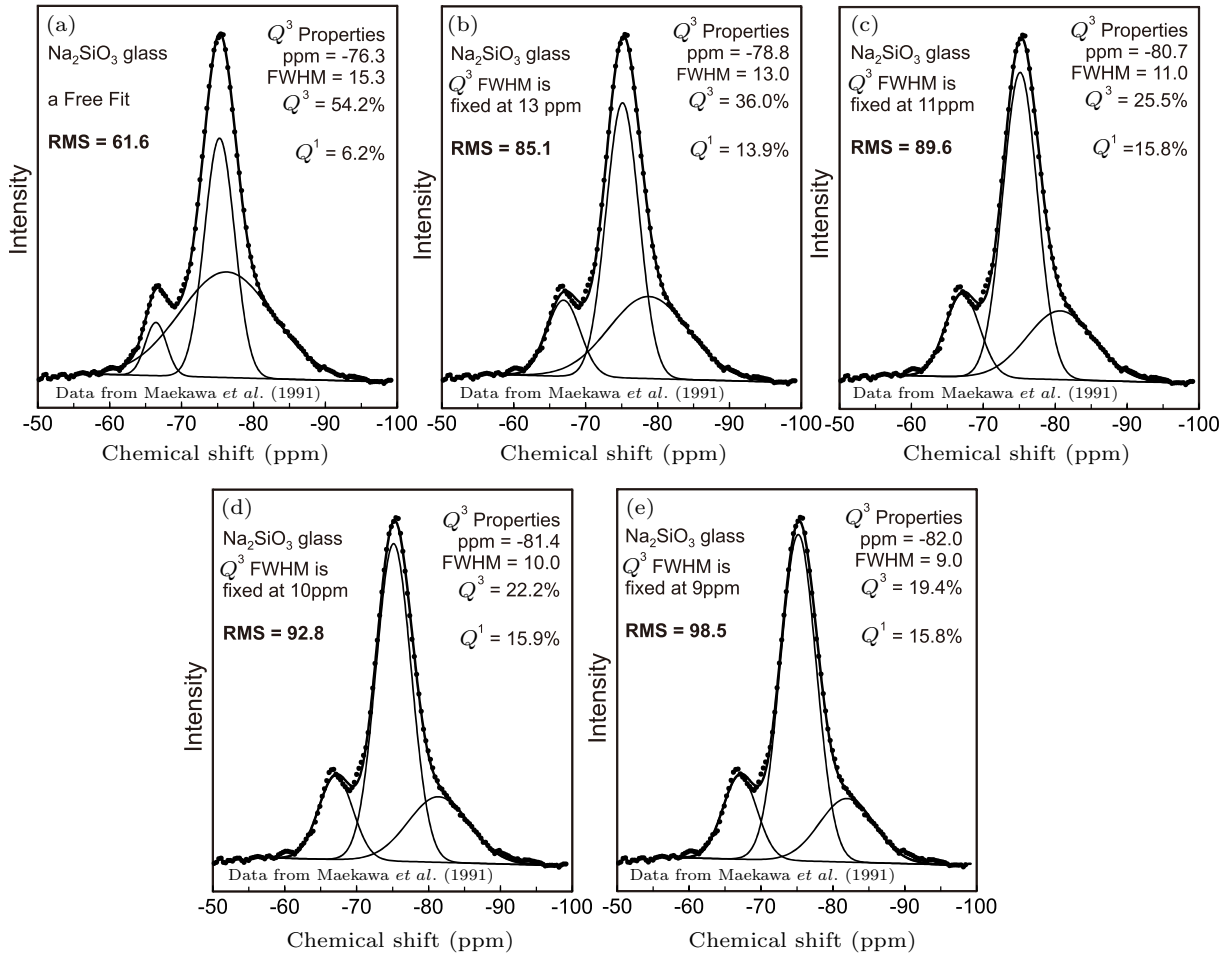


Fig. 1. (a)–(e) Gaussian fits to the digitized ^{29}Si NMR spectrum of the 50 mol% Na_2O glass from Fig. 3 in Ref. [41], using varying Q^3 linewidths. Note that the Q^3 linewidth and intensity decrease systematically from (a) to (e), while the goodness of fit, as represented by the RMS error, increases from 61.6 ((a), free fit) to 98.5 in (e). The Q^3 peak position also shifts systematically from (a) to (e).

Examining the spectral resolution in more detail for the 50 mol% Na_2O glass shown in Fig. 1, the positions and linewidths of the Q^1, Q^2, and Q^3 components are remarkably consistent across studies (all within approximately 1 ppm) between the 1991[41] and 2020[63] datasets (see Table 2 in both works). Specifically, the reported linewidths for Q^1, Q^2, and Q^3 are 4.4 ppm vs. 5.0 ppm, 6.5 ppm vs. 7.2 ppm, and 10.2 ppm vs. 10.0 ppm, respectively, well within typical fitting uncertainties for such partially resolved spectra. It is also important to note that the ^{29}Si NMR spectrum of the 50 mol% K_2O glass measured at 4.7 T by Maekawa (our Fig. 11(a))[41] is, if anything, better resolved than the spectrum of the same composition measured at 14 T by Stebbins in 2020.[63] Indeed, Stebbins does not attempt a full decon-

volution of the 14 T spectrum. There is no clear evidence that even higher magnetic fields would substantially improve the resolution for these systems. For example, Stebbins and coworkers have recently reported high-field (35 T) NMR measurements on silicate glasses for the quadrupolar nucleus ^{25}Mg using the National High Magnetic Field Laboratory (NHMFL) in Florida.[90] However, no corresponding ^{29}Si spectra were reported at 35 T in that study or in other work we are aware of.

Experienced solid-state NMR spectroscopists are well aware that increasing the magnetic field does not necessarily improve the resolution of ^{29}Si NMR spectra of glasses. For silicate glasses, the ^{29}Si NMR linewidth is dominated by chemical shift anisotropy (CSA) and structural disorder, which produces a distribution of chemical shifts. These broadening mechanisms scale with the magnetic field strength; as a result, the linewidth in ppm remains approximately constant. Therefore, higher magnetic fields do not improve and may even degrade the apparent spectral resolution, as observed.

Figures 1(a)–1(e) show immediately that the Q^3 intensity varies strongly with both the assumed Q^3 peak position and linewidth; consequently, neither the Q^3 position nor the linewidth can be determined unambiguously from the data. For example, consider the Q^3 linewidth estimates. Linewidths of approximately 10 ppm from fits to the 40 mol% Na_2O glass have been used in previous studies[41,63] and also by us.[64] A significantly larger assumed Q^3 linewidth shifts the fitted peak to lower ppm and increases the extracted Q^3 area. As the linewidth decreases from Fig. 1(a) to 1(e), the Q^3 peak position shifts and the Q^3 area decreases substantially, approaching the Q^1 area at the smallest linewidth (Fig. 1(e)). The fully unconstrained fit in Fig. 1(a) yields the lowest RMS value (61). However, this fit can be rejected because the resulting Q^3 linewidth is unrealistically large and the peak position is also physically implausible. A low RMS value alone is therefore a misleading criterion for identifying the best fit, despite its widespread use in spectral fitting.

In the remaining four fits (Figs. 1(b)–1(e)), the Q^3 linewidth is fixed to more physically reasonable values (13 ppm, 11 ppm, 10 ppm, and 9 ppm). Under these constraints, four systematic trends are observed: (1) the RMS value increases systematically from 85 (Fig. 1(b)) to 98 (Fig. 1(e)); (2) the Q^3 peak position shifts from 79 ppm to 82 ppm; (3) the Q^3 fraction decreases from 36% to 19%, while the Q^1 fraction remains approximately constant at $\sim$ 15%; and (4) the inferred FO content decreases from $\gg 1$ mol% in Fig. 1(b) to $\ll 1$ mol% in Fig. 1(e).

These results demonstrate that the ^{29}Si NMR spectrum in the Q^2–Q^3 region is too poorly resolved to allow an objective determination of the Q^3 fraction (and hence FO content) without independent constraints on the Q^3 linewidth or position. Further discussion of this spectrum, together with comments on Stebbins' recent fitting results,[63] is provided in Section 2.5. This resolution limitation is common to most ^{29}Si NMR spectra of silicate glasses, and as noted above, there is no evidence that higher magnetic fields significantly improve the resolution. Indeed, this spectrum is better resolved than those of many other alkali and alkaline-earth silicate glasses.[35,46,52]

1.2. Introduction to high resolution O 1s XPS for bulk analysis of silicate glasses

XPS has become an important spectroscopic technique for chemical analysis of solids primarily because it is applicable to all elements except H and He, it generates high-quality spectra with good chemical resolution, and the peaks (including peak widths and shapes) can be readily assigned and quantified.[91–93] However, with the commonly used excitation energy of 1486 eV, the so-called escape depth (corresponding to 63% of the total intensity) is smaller than optimal for bulk analysis. For example, the escape depth has been measured for SiO_2 as 27 Å.[92] The so-called analysis depth (corresponding to 95% of the total intensity) is approximately three times the escape depth — or 81 Å for SiO_2.[91–93] As a result, XPS is usually considered to be primarily a surface-sensitive technique. However, XPS can also provide excellent bulk chemical information for minerals and glasses,[91–93] provided that there is little or no surface contamination or x-ray beam damage. These are the conditions routinely required by the surface science community, but not always by the routine analytical community. For example, in our XPS analysis, glasses are fractured in situ under high vacuum, and care is taken to ensure that little or no adventitious carbon or oxygen is present on the surface. About 5% of the total signal originates from the surface layer;[93] if this surface layer contains oxygen from hydrocarbon contamination, the relative NBO and BO O 1s intensities in the silicate glass will be affected. Our extensive studies show that accurate quantitative analysis of oxygen speciation in silicate glasses is not possible without these precautions. We also find that light Ar ion sputtering of the surface to remove C/O contaminants[94] does not yield satisfactory results. In addition, the relative NBO and BO intensities may be influenced by the nature of the freshly fractured surface. After presentation of the results (see Subsection 2.2), we show that such surface effects do not artificially enhance the measured BO abundances.[35,92]

With the advent of the Kratos Axis Ultra XPS instrument in the late 1990s, featuring improved charge neutralization for non-conducting samples, XPS resolution has improved markedly for materials such as silicate glasses.[95] Equally importantly, the peak shapes are remarkably stable, reproducible, and predictable. Indeed, the O 1s XPS linewidth is 1.25 ± 0.1 eV for FO, NBO, and BO oxygen species in all minerals and glasses studied,[92,95,96] and the line shapes are

consistently 30–50% Lorentzian.[92] To the best of our knowledge, these XPS linewidths and resulting resolution are unmatched in the literature for any modifier oxide–silicate glass system, and represent the intrinsic limit expected for oxygen in SiO_4 tetrahedra in silicate minerals or glasses.[95,96] Constant linewidths and line shapes are also observed in Mössbauer spectra of silicate minerals,[97] but not in NMR or Raman spectra of silicate minerals or glasses.[23–32,41–59,61–64,98,99] As shown in Fig. 1, the ^{29}Si NMR linewidths vary from 5 ppm to >10 ppm in Na silicate glasses;[41,63,64] moreover, the exclusive use of Gaussian line shapes to fit spectra is not always justified. For example, the most recent ^{29}Si NMR spectra of 50 mol% Na_2O glass[63] have been fitted using unspecified Lorentzian contributions rather than purely Gaussian functions.[63] Similarly, although Raman resolution is higher than that of ^{29}Si NMR, Raman peak widths used in fitting glass spectra vary widely (from <40 cm^{-1} to >70 cm^{-1}), and the presence of unassigned "extra" peaks and asymmetries has prevented reliable quantification of Raman peak areas. In contrast, the constant XPS linewidths and line shapes, together with good spectral resolution, make XPS spectra much more straightforward to fit than corresponding NMR and Raman spectra. For transparency, we report peak positions, areas, linewidths, and line shapes without constraints for nearly all spectra, in contrast to common practice in much of the ^{29}Si NMR and Raman literature.

2. Results and discussion

2.1. Large FO in Pb, Ca, and Mg glasses: Consensus from O 1s XPS and ^{29}Si and ^{17}O NMR

Because several papers have questioned the validity of O 1s XPS spectra for obtaining quantitative BO and NBO information in silicate glasses,[61,62,67] we first present O 1s XPS results on Pb silicate glasses, together with ^{29}Si and ^{17}O NMR results,[65,66,88] to demonstrate that: (1) O 1s spectra provide accurate and transparent determinations of FO, BO, and NBO in these glasses; (2) these results are consistent with the Q-species distributions derived from ^{29}Si NMR[66] and ^{17}O NMR;[88] (3) the equilibrium description given by Eqs. (2) and (3) holds over a wide compositional range, yielding >15 mol% FO at 66.7 mol% PbO, decreasing to approximately ~ 1 mol% FO at 30 mol% PbO.

In Fig. 2, we present O 1s XPS spectra[65,69] (acquired using a modern Kratos Axis Ultra spectrometer) for four PbO compositions, ranging from 50 mol% PbO in Fig. 2(a) to 76.7 mol% PbO in Fig. 2(d). It is important to emphasize that clean, freshly fractured surfaces and an effective charge compensation protocol are required to achieve narrow linewidths of approximately ~ 1.2 eV and consistent symmetric line shapes for all oxygen species in our non-conducting mineral and glass systems.[92,95,96] The narrow O 1s peaks (linewidths ≤ 1.22 eV) in Figs. 2(a)–2(c) can be reliably fitted using two peaks of identical width and shape at approximately 530 eV and 531.5 eV. No fitting parameters are constrained in these O 1s spectral decompositions. These two components are assigned to NBO and BO oxygen species, respectively, since NBO possesses higher valence electron density than BO due to charge donation from Pb.[36,37,91]

For the 76.7 mol% PbO spectrum in Fig. 2(d), two clear indications suggest an additional contribution within the NBO envelope: (1) the NBO peak maximum shifts by approximately 0.5 eV toward lower binding energy, and (2) the NBO linewidth increases from 1.22 eV to 1.67 eV. Under these conditions, the NBO region can be resolved into two peaks of identical width (1.22 eV), corresponding to NBO at 529.8 eV and FO at 529.0 eV, respectively. In the spectra shown in Figs. 2(a)–2(c), the NBO envelope contains both NBO and a much smaller FO contribution that is not resolved as a separate peak.

From the areas of the two large peaks and assuming equal photoionization cross sections for the oxygen species,[91] the mole fraction of BO (X_{BO}) (solid circles) can be determined as a function of X_{PbO} in Fig. 2(e). Before discussing these XPS-derived values and the NMR results obtained from ^{29}Si spectra[66] (open squares), it is useful to consider the short dashed line representing X_{BO} for the limiting case $K_3 = \infty$. This line corresponds to the absence of FO, with only BO and NBO present in the system. The expected X_{BO} values for stoichiometric SiO_2, $PbSi_2O_5$, $PbSiO_3$, and Pb_2SiO_4 are 1.0, 0.60, 0.33, and 0, respectively, all of which lie on the dashed line in Fig. 2(e). For example, in $PbSiO_3$ there is one BO and two NBO per Si, giving $X_{BO} = 1/3 \approx 0.33$. The ^{29}Si NMR-derived X_{BO} values[66] for glasses with $X_{PbO} < 0.4$ lie very close to the $K_3 = \infty$ line. However, for $X_{PbO} > 0.4$, the X_{BO} values from both techniques systematically lie above this limiting line. In particular, at $X_{PbO} = 0.67$, the dashed-line model predicts $X_{BO} = 0$, whereas the experimental O 1s XPS[65,69] and ^{29}Si NMR[66] results give $X_{BO} = 0.19$ and 0.15, respectively (see below for the derivation of X_{BO} from the Q species obtained from the ^{29}Si NMR spectra). The ^{17}O NMR spectra show excellent resolution of peaks from BO, NBO, and FO;[88] however, no fits to the resolved spectra are performed, mainly due to the unusual peak shapes arising from the quadrupolar ^{17}O nucleus.[67,88] Nevertheless, a large resolved FO peak is clearly observed, and the authors report $X_{FO} = X_{BO} \approx 0.135$.[88] The two NMR and O 1s XPS results indicate a significant X_{FO}, implying that reaction (2) does not proceed to completion and that K_3 is finite. Most importantly, the substantial X_{FO} contribution in all cases demonstrates that polymerization via Eq. (2) occurs and that FO is a critical species in the glass. Of course, disproportionation is not possible for a Q^0 species.

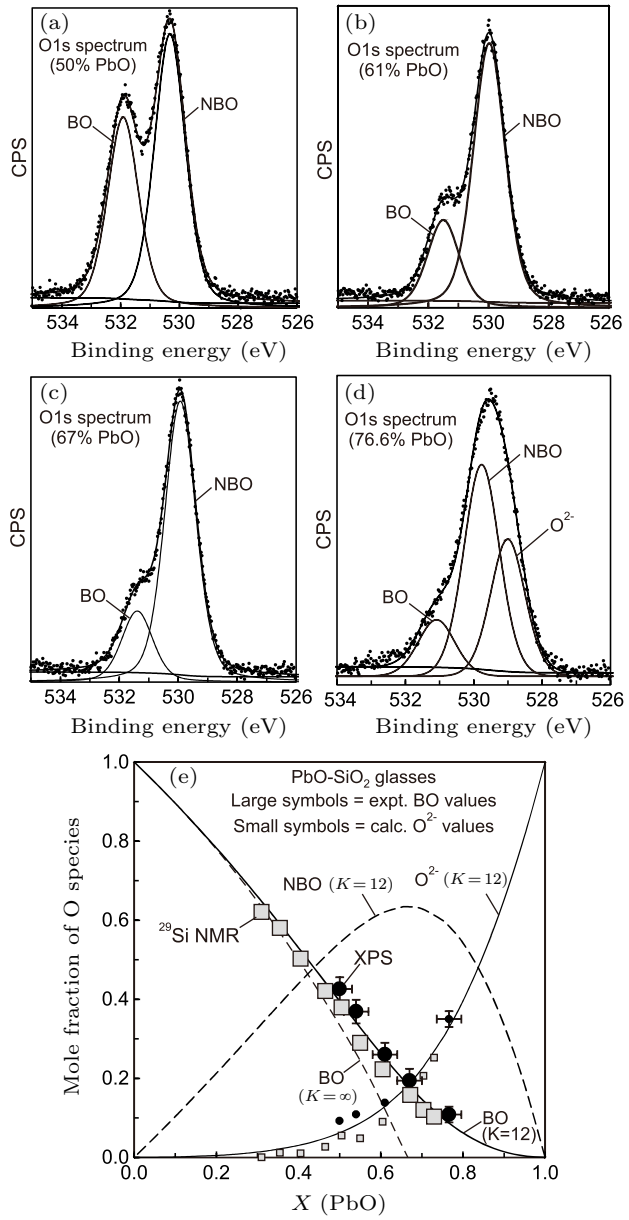


Fig. 2. O 1s XPS spectra of four Pb silicate glasses of composition: (a) 50 mol% PbO, (b) 61 mol% PbO, (c) 67 mol% PbO, and (d) 76.7 mol% PbO.[65,69] (e) shows the mole fractions of BO, NBO, and FO (X_{BO}, X_{NBO}, and X_{FO}, respectively), with estimated errors (±0.02) indicated by the size of the squares and circles, plotted as a function of the mole fraction of PbO (X_{PbO}). Results from O 1s XPS[65,69] (black circles) and ^{29}Si NMR[66] (shaded squares) are shown. The four curves are: (1) the expected X_{BO} for $K_3 = \infty$ (short-dashed curve); (2) the best overall fit for $K_3 = 12$ (solid curve), obtained from the X_{FO} and X_{BO} values derived from the fit to the 76.7 mol% PbO composition and passing through the experimental squares and circles; (3) X_{NBO} for $K_3 = 12$ (long-dashed curve); and (4) X_{FO} for $K_3 = 12$ (solid line). The small squares and circles correspond to X_{FO} values calculated from the difference between the two X_{BO} curves.

At $X_{PbO} = 0.67$, the XPS results show that $X_{BO} \sim 0.19$ (Fig. 2(e), large black circle). What is K_3 for this sample? From Eq. (2), and noting that $X_{BO} = X_{FO} \approx 0.19$ for the 66.7 mol% PbO sample, while oxygen mass balance gives $X_{BO} + X_{NBO} + X_{FO} = 1$, we obtain $X_{NBO} \approx 0.62$, and hence $K_3 = 10.7$. The value of K_3 is rather sensitive to X_{BO}. For example, if $X_{FO} = 0.16$, then $K_3 = 18.0$. A value of $K_3 = 12$ was used for the solid X_{BO} curve, which provides a good visual fit within the uncertainties assigned to the X_{BO} values from O 1s XPS and ^{29}Si NMR (Fig. 2(e)). The accuracy of the K_3 value cannot be precisely evaluated at this stage, but it likely lies between 10 and 20.

The X_{FO} values for $K_3 = 12$ are also plotted as a solid curve at the bottom of Fig. 2(e). X_{FO} decreases rapidly with decreasing X_{PbO}; $X_{FO} \approx 0.07$ (7% FO) at 50 mol% PbO, and $X_{FO} \approx 0.01$ (1% FO) at 30 mol% PbO. The equilibrium treatment therefore requires appreciable (mol%) FO even at $X_{PbO} = 0.3$ for K_3 between 10 and 20. It is also important to note that the difference between the two BO curves (ΔX_{BO}) directly yields X_{FO} at all X_{PbO}. This is most clearly seen for the 66.7 mol% PbO glass, where $\Delta X_{BO} = 0.19$, giving $X_{FO} = 0.19$. At 50 mol% PbO, $\Delta X_{BO} = 0.07$.

The Q-species distributions from ^{29}Si NMR (and, as shown later, Raman) can be used to determine the abundances of NBO and BO in a glass using the following mass-balance equations (normalized to O_{total}/Si)

$$N_{BOt} = 2X_{Q4} + 1.5X_{Q3} + 1.0X_{Q2} + 0.5X_{Q1}, \tag{8}$$

$$N_{NBOt} = 1.0X_{Q3} + 2.0X_{Q2} + 3.0X_{Q1} + 4.0X_{Q0}, \tag{9}$$

$$N_{BOt} + N_{NBOt} + N_{FO} = N_{Ototal}/\mathrm{Si}, \tag{10}$$

$$X_{BOt} + X_{NBOt} + X_{FO} = 1. \tag{11}$$

For example, for the 67 mol% PbO glass, the ^{29}Si NMR[66] yields $X_{Q3} = 0.05$, $X_{Q2} = 0.31$, $X_{Q1} = 0.52$, and $X_{Q0} = 0.12$. Substituting into Eqs. (8) and (9) gives $N_{BOt} = 0.64$ and $N_{NBOt} = 2.72$. At this composition, $N_{FO} = N_{BOt} = 0.64$, and $N_{Ototal}/\mathrm{Si} = 4$ as expected for Pb_2SiO_4. Thus, X_{BO}, X_{NBO}, and X_{FO} are obtained by dividing by four, yielding 0.16, 0.68, and 0.16, respectively, as shown in Fig. 2(e). For $PbSiO_3$, the ^{29}Si NMR[66] gives $X_{Q4} = 0.06$, $X_{Q3} = 0.30$, $X_{Q2} = 0.51$, and $X_{Q1} = 0.13$, yielding $N_{BOt} = 1.14$ and $N_{NBOt} = 1.71$, with a total of 2.85, so $N_{FO} = 0.15$ ($N_{Ototal} = 3.0$). The resulting X_{BO}, X_{NBO}, and X_{FO} values are obtained by dividing by three, i.e., 0.38, 0.57, and 0.05, respectively. Note that this X_{BO} value (0.38) is 0.05 larger than the $K_3 = \infty$ value of 0.33, as expected. The FO value is slightly smaller than that obtained from $K_3 = 12$ or from XPS. As shown above, this equilibrium treatment enforces a rigorous evaluation of oxygen mass balance,[35,83–85] which has often been overlooked in the NMR and Raman literature. Using oxygen mass balance makes it evident that the X_{BO} values cannot lie below the dotted curve, because this would lead to negative FO values, which is physically impossible. Figure 2(e) should be essential for all spectroscopists studying silicate glasses, as it illustrates both oxygen mass balance and equilibrium among the three oxygen species.

Our detailed analysis of FO contents in alkaline-earth silicates from literature ^{29}Si and ^{17}O NMR and Raman

studies[70–73] on Mg, Ca, and Mg/Ca glasses, including orthosilicates (66.7 mol% *M*O) and metasilicates (50 mol% *M*O),[69] shows large FO concentrations: 5–10 mol% at 66.7 mol% and 1–2.6 mol% at 50 mol%, with associated NBO/Si values that are substantially below the stoichiometric crystalline values of 4 and 2, respectively.[100] MD calculations on these glasses also give large but variable FO values.[69] For example, MD calculations on Mg_2SiO_4[101–103] yield X_{FO} values of 5%, 15%, and 16%, corresponding to a large range of K_3 values (330, 21.8, and 18.0, respectively).

For 66.7 mol% *M*O Pb, Ca, and Mg glasses–compositions that nominally suggest only Q^0 species (as in orthosilicate crystals)–appreciable Q^1 and Q^2 species are nevertheless present. This can only arise via polymerization as in Eq. (4). Two additional results are worth noting. An ^{17}O NMR[104] study on a 56 mol% CaO glass concluded that there was no appreciable FO based on measured BO and NBO fractions,[69] without considering oxygen mass balances. However, using the mass balance relations in Eqs. (10) and (11), the inferred FO would range from 1.7% to 3.2%, depending on the choice of BO values.[69,104] Conversely, a well-resolved ^{17}O NMR spectrum of a 45 mol% BaO silicate glass yields unphysical negative FO values when using the reported BO assignments.[104] It has been difficult to quantify well-resolved ^{17}O NMR spectra due to variable linewidths, irregular peak shapes arising from the quadrupolar nature of the ^{17}O nucleus, and shifts in relative peak positions with changes in magnetic field.[21,89] As a result, Lee and Kim[88] did not fit their well-resolved ^{17}O NMR spectra of Pb silicates, and Stebbins[63] did not attempt to fit or quantify the resolved ^{17}O NMR spectrum of the 50 mol% K_2O silicate glass.

2.2. Mol% FO from the O 1s XPS spectra of Na and K silicate glasses

Figures 3 and 4 show the O 1s XPS spectra and the X_{BO} plots for our Na[20,64] and K silicate glasses[21,35,68,87] over a wide range of compositions, along with X_{BO} values from the only other O 1s XPS study with reasonable resolution.[105] The counting times for these spectra are longer than for the Pb spectra in Fig. 2, and as a result the statistics in Figs. 3 and 4 are much better than in Fig. 2. Excellent fits are obtained in all cases to the two resolved O 1s peaks without constraints, and all fitting parameters are listed in the above six papers. The assignment of the two resolved peaks is the same as for the Pb spectra — BO peak at ∼ 532 eV and NBO + FO peak at ∼ 530 eV. As expected from Eq. (2), the relative intensity of the BO peak decreases as the mol% Na_2O and K_2O increases in Figs. 3 and 4. Note that the separation of the two peaks increases in the order Pb (∼ 1.5 eV) < Na (∼ 2.0 eV) < K (∼ 2.2 eV) — as the electronegativity (EN) of the cation decreases from 1.87 (Pb) to 0.93 (Na) to 0.82 (K).[106] This difference is mostly due to the decrease in O 1s BE of the NBO atoms due to greater charge transfer of electrons in the order Pb < Na < K, which results in a decrease in the NBO BE from 530.3 eV to 530.0 eV to 529.5 eV, respectively.

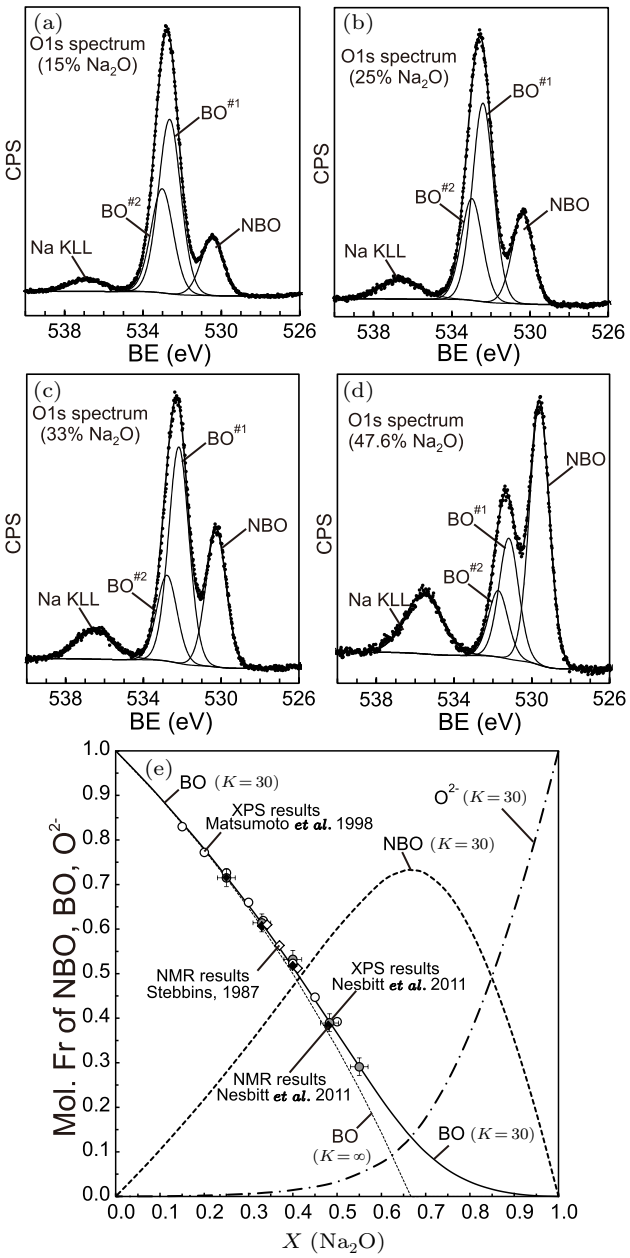


Fig. 3. O 1s XPS spectra of four Na silicate glasses of composition: (a) 15 mol% Na_2O, (b) 25 mol% Na_2O, (c) 33 mol% Na_2O, and (d) 47.6 mol% Na_2O.[20,64] (e) shows the plot of mole fraction of BO, NBO and FO (X_{BO}, X_{NBO} and X_{FO} respectively) versus the mole fraction of Na_2O (X_{Na_2O}) from our experimental O 1s XPS results (black circles),[20,64] Matsumoto's O 1s XPS results (open circles),[104] as well as ^{29}Si NMR results from Stebbins[32] (open diamonds) and Nesbitt *et al.*[64] (open circles). See Subsection 2.2 for more details. The errors on our O 1s XPS results are given by the error bars on the black circles. The four curves are: (1) the expected X_{BO} for K_3 = infinity (light short-dashed curve); (2) the best overall fit X_{BO} for $K_3 = 30$ (solid curve) which goes through all the X_{BO} values from XPS and NMR; (3) X_{NBO} for $K_3 = 30$ (solid dashed curve); and (4) X_{FO} for $K_3 = 30$ (dash-dot line).

The BO peak is substantially broader than the NBO peak by ∼ 0.2 eV for the Na spectra[21,64] and ∼ 0.3 eV for the K spectra,[87] suggesting strongly that the BO peak is composite, due to M–BO interactions discussed below. Fits with two and

three BO peaks for the Na and K spectra,[20,21] respectively (Figs. 3(a)–3(d) and 4(a)–4(d)), constraining each linewidth to the NBO linewidth of ~ 1.2 eV, are shown in Figs. 3(a)–3(d) and 4(a)–4(d). Because these BO peaks are very close together, the relative intensity of these BO components cannot be determined quantitatively; but most importantly, the X_{BO} values are not significantly affected by the number of BO peaks included. Such fits of strongly overlapping peaks are only reasonable when there is exceptional reproducibility of the linewidths and lineshapes. Indeed, these O 1s spectra show exceptional reproducibility. Except for the 10 mol% K_2O glass, the linewidths of the narrower NBO peak for all Na and K glasses are < 1.3 eV, and most are very close to 1.2 eV. These narrow linewidths and constant lineshapes are maintained over many hours of x-ray exposure, as shown in Table 1 of Ref. [21]. These widths are all considerably smaller than the somewhat variable NBO widths (1.4–1.6 eV in Matsumoto's paper[104]) and the even larger NBO widths in earlier O 1s XPS studies[36,37] using older conventional charge compensation techniques. Moreover, the 1.2 eV widths are very close to the minimum linewidth expected for a SiO_4 moiety due to vibrational broadening.[96]

As stated above, the broadening of the BO peak is due to interactions of Na and K with BO, as also seen in crystalline Na and K silicates such as $Na_2Si_2O_5$[107] and $K_2Si_2O_5$.[108] For example, in the K glass spectra, the three BO peaks probably arise from three distinct BO environments associated with different numbers of K atoms bonded to BO (e.g., 0, 1, and 2). These peaks are separated by ~ 0.5 eV (see Fig. 3(d)), compared to the separation between BO and NBO of 2 eV.[21] The interaction of each Na or K with a BO results in a more negatively charged BO and a lower O 1s binding energy (BE). In support of this interpretation, crystalline $K_2Si_2O_5$[108] contains three types of BOs. It is important to emphasize that the calculated X_{BO} values are not substantially affected by the number of BO peaks used in the fit. For example, Table 1 in Ref. [21] for the K glasses shows that the X_{BO} values obtained from one-BO-peak and three-BO-peak fits differ by within 0.4% absolute for four glasses (e.g., 0.840 and 0.843 respectively for the 15 mol% K_2O glass in Fig. 4(b)), and within 1% absolute for the other two glasses (e.g., 0.644 and 0.653 respectively for the 32 mol% K_2O glass in Fig. 4(d)). Similarly, for the Na glasses,[21,64] the X_{BO} values are also within 1% absolute for one- and two-peak BO fits: e.g., 0.737 and 0.731 for the 25 mol% Na_2O glass, and 0.544 versus 0.536 for the 40 mol% Na_2O glass.

We also corrected for small observed increases in X_{BO} with x-ray exposure time. The BO fraction was plotted against exposure time T, and the X_{BO} values for each sample were extrapolated back to $T = 0$.[20,21] For most samples, this extrapolation changes X_{BO} by much less than 1% absolute compared to the first recorded spectrum. For example, for the two-BO-peak fit to the 25 mol% and 40 mol% Na_2O spectra, X_{BO} decreases from 0.731 (first spectrum, see above) to 0.724 (extrapolated value); and for the 40 mol% spectrum, X_{BO} decreases from 0.536 to 0.528. These "$T = 0$" values are those plotted in Figs. 3 and 4. The estimated errors in both composition and X_{BO} are given by the error bars in Figs. 3(e) and 4(e).

Are these errors realistic? For siliceous glasses with $X_{Na_2O} < 0.3$ and $X_{K_2O} < 0.2$, the X_{BO} values from both our results and those of Matsumoto[104] lie directly on the solid and short-dashed lines required by Eq. (2). This provides strong evidence that the XPS method yields reliable X_{BO} values. For $X_{Na_2O} > 0.3$ and $X_{K_2O} > 0.2$, both data sets from these two independent groups deviate systematically above the short-dashed line for $K_3 = \infty$, strongly indicating that K is finite and that mol% FO is present in these samples. For example, for six different K glasses with 26–34 mol% K_2O, the FO content varies from 1.5% to 3.5% (average 2.2% for all six, and 2.0% excluding the 3.5% outlier), with an uncertainty of $\pm 1\%$ on each value.[35] This provides strong evidence that > 1 mol% FO is present at ~ 30 mol% K_2O. In contrast, the X_{BO} data for comparable 25–30 mol% Na_2O glasses does not show a significant deviation from the short-dashed line,[21,64] suggesting that FO is smaller in Na glasses of comparable composition than in K glasses.

Previous publications,[61–63,67] as well as a referee of this paper, have argued that surface sensitivity in XPS could lead to an overestimation of BO, which we attribute instead to FO. We addressed this concern in earlier work,[35,92] but it is worth reiterating with additional evidence from Greaves *et al.*[109] He corroborates our previous conclusion that freshly fractured glass surfaces are, if anything, Na-rich (i.e., NBO-rich), because weak Na–O bonds (Na–O bond energy of 239 kcal/mol) are more easily broken than Si–O bonds (Si–O bond energy of 798 kcal/mol[106]). Greaves[109] states: "*Certainly there is much evidence from a variety of studies for the large alkali content of freshly fractured glass surfaces*". See also Fig. 8 in that work. A similar M–O (M = Pb, Mg, Ca) enrichment would be expected for divalent cations. For an NBO-rich surface, the measured X_{NBO} would, if anything, be slightly larger than the bulk value. Since $X_{BO} + X_{NBO} = 1$, an increase in X_{NBO} necessarily implies a decrease in X_{BO}, not an increase in X_{BO} as claimed by critics.[61–63,67] If anything, this implies that we are underestimating the BO and FO amounts!

There are three observations that show that such a NBO-rich surface layer does not affect our bulk X_{BO} measurements within the quoted errors of 0.02. First, for the Pb glasses, there is good agreement between the O 1s XPS results and the ^{29}Si and ^{17}O NMR results: all techniques give large FO contents at ≥ 50 mol% PbO as shown above. Second, for the Na and K glasses at < 30 mol% Na_2O or < 20 mol% K_2O, the X_{BO}

results agree with the theoretical results using Eq. (3), assuming that K_3 = infinity. Third, the O 1s XPS results for the Na and K glasses agree with the properly assigned and interpreted ^{29}Si NMR and Raman results (see below). In summary, the intensity from a possible NBO surface signal does not affect our bulk analysis significantly.

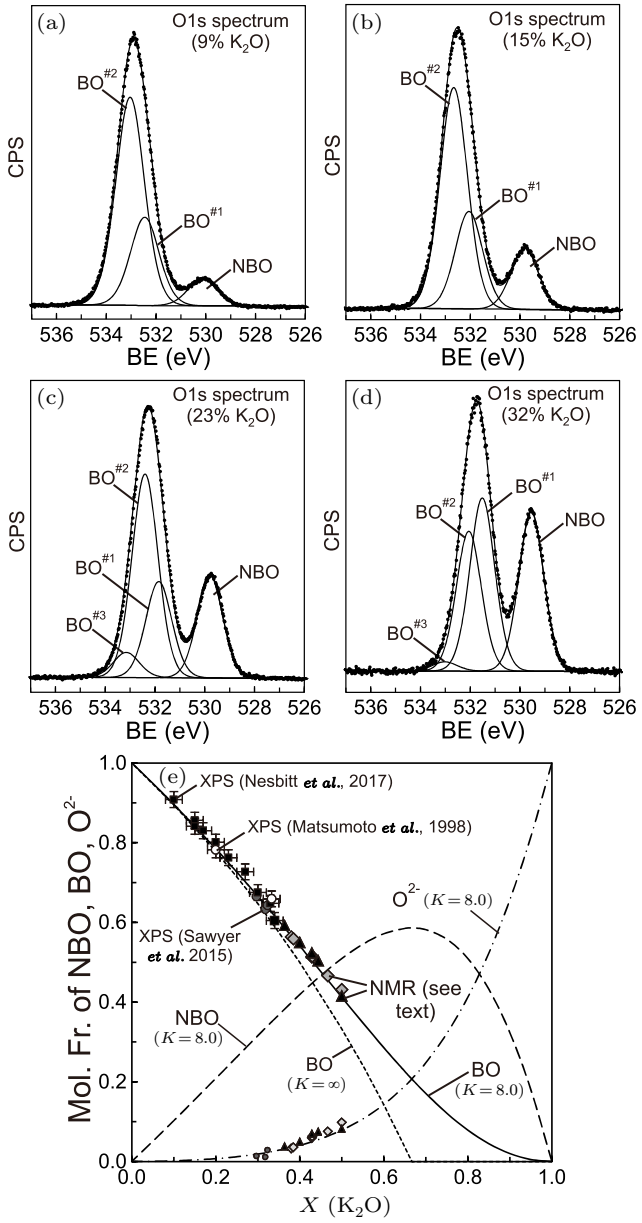


Fig. 4. O 1s XPS spectra of four K silicate glasses of composition: (a) 9 mol% K_2O, (b) 15 mol% K_2O, (c) 23 mol% K_2O, and (d) 32 mol% K_2O.[21,35] Figure 3(e) shows the plot of mole fraction of BO, NBO and FO (X_{BO}, X_{NBO} and X_{FO} respectively) versus the mole fraction of K_2O (X_{K_2O}) from our experimental O 1s XPS results (black circles) (from Fig. 9 in Ref. [35]) and Matsumoto's O 1s XPS results (open circles),[104] as well as ^{29}Si NMR results from Malfait[46] (shaded diamonds) and Maekawa[41] (black triangles) after reassignment of the NMR spectra as detailed in Subsection 2.4. Without the reassignment, all the ^{29}Si NMR results lie on the dashed curve for K_3 = infinity. The errors on our O 1s XPS results are given by the error bars on the black circles. The four curves are: (1) the expected X_{BO} for K_3 = infinity (short-dashed curve); (2) the best overall fit X_{BO} for $K_3 = 8$ (solid curve) which goes through all the X_{BO} values from XPS and NMR; (3) X_{NBO} for $K_3 = 8$ (long-dashed curve); and (4) X_{FO} for $K_3 = 8$ (dash-dot line). The smaller squares and circles are the X_{FO} values calculated from the difference between the two X_{BO} curves.

Some of the X_{BO} values derived from ^{29}Si NMR data[32,41,64] (e.g. the X_Q values from Table 1) are also plotted on Figs. 3 and 4 after converting the Q species distributions to N_{BOt} (Eq. (8)) and X_{BO} ($= N_{BOt}/O_t$). For example, for the 41 mol% Na_2O sample (third and fourth glasses in Table 1), $N_{BOt} = 1.37$ and $O_t = 2.70$ ($Na_{1.40}SiO_{2.70}$), giving $X_{BO} = 1.37/2.70 = 0.507$, which is 0.026 (2.6 mol% FO) larger than X_{BO} (and $= X_{FO}$) for the short-dashed line for K_3 = infinity (0.481). These values are within the round-off error of the 2.8 mol% FO given in Table 1. The solid lines give a good visual fit to the O 1s XPS data and most of the ^{29}Si NMR data. For the 40 mol% Na_2O glass, the four X_{BO} results (two from XPS and two from ^{29}Si NMR) given in Fig. 3 are in reasonable agreement and all show mol% FO. These solid lines are obtained using a K_3 value of 30 and 8 for Na and K glasses, respectively. The K_3 value for the Na glasses is larger than the $K_3 = 15$ given in the initial publication.[64] As pointed out by Stebbins,[63] we should have used the actual quoted composition (47.6 mol% Na_2O) rather than the nominal composition of 50 mol% Na_2O, and this has been corrected in Fig. 3 for both the XPS[20] and ^{29}Si NMR.[64] This change results in a smaller FO by ~ 2 mol% from the earlier paper[64] with a larger K_3; however, FO is still 1.8 mol% (XPS) (Table 3 in Ref. [64]) and 0.6 mol% (NMR). Similarly, accurate compositions for the K glasses were essential to obtain accurate FO and K_3 values.[35] As indicated in the discussion of the Pb results in Subsection 2.1 above, the K_3 values have large errors; but they do indicate strongly that: (1) in both Na and K glasses, mol% FO is present for 30–40 mol% glasses, and (2) that K_3 for the K glasses is significantly smaller than for Na glasses, and is comparable to the K_3 for the Pb glasses.

The X_{BO} and FO values from the ^{29}Si NMR results for the ~ 40 mol% Na_2O glass strongly indicate mol% FO from several studies (Table 1[32,41,42,64,83]). Unlike other Na silicate glasses, the 40 mol% Na_2O glass gives two intense peaks with reasonable resolution (Fig. 5(a)) making it possible to fit the large Q^2 and Q^3 peaks without applying constraints to Gaussian peaks and derive quantitative Q^2 and Q^3 (and Q^4 from static ^{29}Si NMR) and X_{BO} from free fits without "adjustments".[83] In contrast, the 33.3 mol% and 50 mol% Na_2O glasses (e.g. the original spectrum and fit[41] shown in Fig. 5(b)) have only one intense peak with two small overlapping peaks.[41,63,64] As we discussed in Subsection 1.1 and later in Subsection 2.5, it is not possible to obtain an objective fit and quantitative Q species content from this spectrum.[63]

The Q species abundances are listed in Table 1 from four ^{29}Si NMR studies of the 40 mol% Na_2O glass. There are three important observations: (1) the Q species distributions are in good agreement with each other; (2) they all result in between 1.0 mol% and 2.8 mol% FO; and (3) the BO values derived in

Fig. 3e are in agreement with the two O 1s XPS results.[64,104] For example, the average FO for the four NMR studies in Table 1 is 1.9 mol%, and the XPS results give 2.0 mol% for the nominal composition (40%) and 3.0 mol% for the analyzed composition (41.1%).[64]

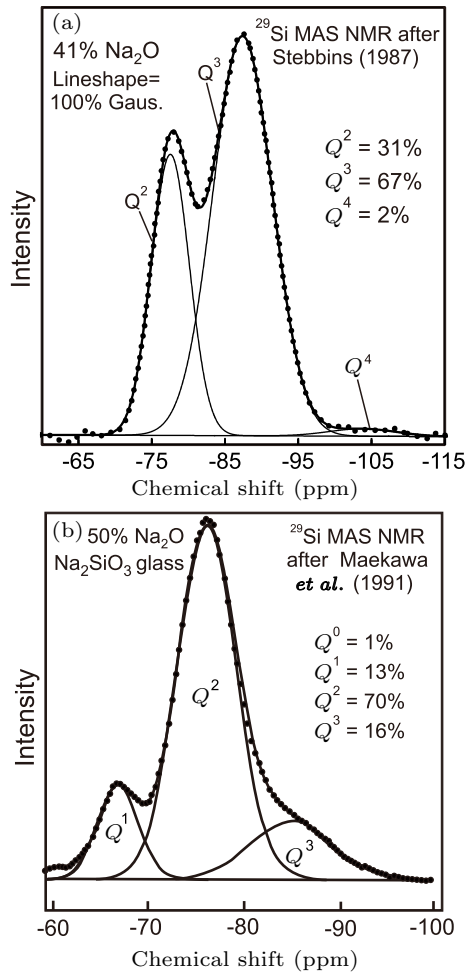


Fig. 5. The ^{29}Si MAS NMR spectra (a) 41 mol% Na_2O glass, and (b) 50 mol% Na_2O glass redrawn from the original publications (Refs. [32] and [41], respectively). The fit to the spectrum in (a) is new, and the Q species abundances are in good agreement with other NMR results (Table 1). The fit to the spectrum in (b) is taken from Maekawa's original spectrum in his Fig. 3,[41] which gives no appreciable FO (Table 2).

Table 1. Q species abundances in 40/41 mol% Na_2O glasses from ^{29}Si NMR spectra[a].

Glass/Melt	Q^4	Q^3	Q^2	Q^1	K_D	FO
Mol% Na_2O	%	%	%	%		Mol%
41.1%[32]	2.0	70.6	27.4	0	0.011[32]	2.8
40.0%[41]	2.0	68	29	1	0.013	1.0
40.0 [42]	1.6	68.2	30.2	0	0.013	1.1
41.1[64]	3.5	67.7	28.8	0	0.022	2.8
Average	2.4	68.8	28.8	0.0	0.014	1.9
Std. Deviation	1.0	1.6	1.4	0	0.005	0.9

(a) The table has the same numbers as in Ref. [83], but the FO values are quoted here for the first time.
Q^4 — measured from static ^{29}Si NMR.[32] We calculated Q^2 and Q^3 using the quoted $K_D = 0.011$ and $Q^2 + Q^3 + Q^4 = 100$ (see Eqs. (12) and (13) of text)

The first, and best, ^{29}Si NMR spectrum (Table 1) for a $\sim$ 40 mol% Na_2O glass was published by Stebbins in 1987 (Fig. 5(a))[32] using an enriched ^{29}Si glass. He quoted the Q^4 abundance (from the static ^{29}Si NMR spectrum), but he did not quote Q^2 and Q^3 abundances; and it is important to show how we obtained[83] the Q^2 and Q^3 values in Table 1. Although Stebbins did not show a fit to the spectrum, he obviously measured the Q^2 and Q^3 abundances because he quoted an equilibrium constant K_D (= 0.011) for the disproportionation reaction (Eq. (7a))

$$2Q^3 \Leftrightarrow Q^2 + Q^4,$$
$$K_D = [X_{Q2}][X_{Q4}]/[X_{Q3}]^2. \tag{12}$$

With the mass balance equation

$$X_{Q2} + X_{Q3} + X_{Q4} = 1, \tag{13}$$

and $X_{Q4} = 0.02$, we obtain two equations (Eqs. (12) and (13)) in two unknowns, X_{Q2} and X_{Q3}. Solving the resulting quadratic equation gives $X_{Q2} = 0.274$, $X_{Q3} = 0.706$, and $X_{Q4} = 0.02$ (Table 1). To obtain the X_{FO} for these 41 mol% Na_2O glasses, we use Eq. (14), resulting from the O mass balance[36]

$$X_{FO} = 1 - (N_{Q\,total}/N_{Ototal}). \tag{14}$$

As previously stated for Eqs. (8)–(11), N_{Ototal} is the number of moles of O per mole of Si. Therefore, the composition of the glass is expressed as $Na_{1.40}SiO_{2.70}$, and $N_{Ototal} = 2.70$. Then N_{Qtotal} is given by the sum of the NBO and BO contributions in Eqs. (8) and (9)

$$N_{Q\,total} = 3.0X_{Q2} + 2.5X_{Q3} + 2.0X_{Q4}. \tag{15}$$

Substituting the above X_Q values into Eqs. (14) and (15) gives

$$X_{FO} = 1 - \{3.0X_{Q2} + 2.5X_{Q3} + 2.0X_{Q4}\}/2.70, \tag{16}$$
$$X_{FO} = 1 - \{2.627/2.70\} = 1 - 0.972 = 0.028. \tag{17}$$

The mass balance shows that the total O from the Q species is 2.63, which is less than the total O in the sample (2.70). This discrepancy must be due to the presence of FO. Because Stebbins did not consider the O mass balance, he assumed that FO was 0. This significant value of 2.8 mol% FO, demonstrating the importance of polymerization, was already implicit in 1987! Note that the other FO values in Table 1 lie between 1.0 and 2.8 mol%.

If one relies solely on disproportionation, the above O 1s XPS and ^{29}Si NMR (and later Raman spectra) cannot be fully explained. Moreover, assuming FO = 0 mol% in silicate compositions with < 60 mol SiO_2 is no longer a viable stance, and the depolymerization reaction must be considered in combination with the oxygen mass balance. Furthermore, recent papers have negated oxygen equilibria and undercut further development of the analysis of ^{29}Si NMR spectra by reporting values

for Q^n and O species without explanation of the fitting procedure and assumptions used to obtain them.[62,63] This amounts to a step backwards in the quantitative data reduction for any technique and should cause concern for ^{29}Si NMR users.

The X_{BO} results shown in Fig. 4(e) for the K_2O glasses are more significant because of the small K_3 of 8, with FO $\geq$ 1 mol% at 30 mol% K_2O, projected to increase to $\geq$ 7 mol% at 50 mol% K_2O (solid line). We have argued strongly in our 2015 papers[35,68] that the ^{29}Si NMR spectrum of the 50 mol% glass should be re-assigned (see Subsection 2.4), and this re-assignment yields the X_{BO} values given in Fig. 4(e) (solid triangles[41] and shaded diamonds[46]) from the two major ^{29}Si NMR studies. They lie right on the line for $K = 8$. With the publication of high-quality Raman spectra of the 50 mol% K_2O glass in 2023,[76] combined with the firm assignment of Raman spectra of Na and Ba glasses,[83–85] we can now show strong new evidence that our proposed ^{29}Si NMR re-assignment of the 50 mol% K_2O spectrum is justified. First, we address the new advances in Raman spectroscopy of silicate glasses which lead to firm assignments of the Na and Ba silicate spectra in the next section, before returning to the assignment of the 50 mol% K_2O ^{29}Si NMR spectrum in Subsection 2.4.

2.3. Towards quantitative Raman spectroscopy: Assignment, and quantitative analysis for FO for 40 mol% Na_2O, BaO and K_2O silicate glasses and melts

Franz and Mysen[52] and McMillan *et al.*[110] suggested that the Raman spectra of silicate glasses could be quantified by comparing the better resolved Raman spectra directly with the ^{29}Si NMR spectrum of the same composition. Franz and Mysen[52] showed the two spectra of $CaSiO_3$ glass (Figs. 6(a) and 6(b)) and proposed that the Raman cross sections for the three Q species could be obtained from the peak areas, assuming that the ^{29}Si NMR cross sections were the same for all Q species. Unfortunately, there was no consensus on the assignment of the high-energy peak (labelled Q^3 in Fig. 6(b)[52]) at $\sim$ 1050 cm^{-1}; and the ^{29}Si NMR spectrum was too poorly resolved (more poorly resolved than Fig. 1) to obtain quantitative areas for the three peaks. Although the two spectra (Fig. 6) are qualitatively similar (an intense Q^2 peak with two weaker peaks on either side), the high-energy peak at $\sim$ 1050 cm^{-1} was assigned to something other than the obvious Q^3 peak, mostly because "conventional wisdom" dictated that the Q^3 intensity could not be larger than Q^1 based only on disproportionation in a 50 mol% glass (see Eq. (7b)). The 1050 cm^{-1} peak in Fig. 6(b) (and many other Raman spectra) was assigned to a peak not related to a symmetric stretch of a Q species, for example, to an unspecified Si–BO peak sometimes labeled "Si–O"[51–54,57,74,75] or a second Q^2 peak.[58,59,76] (see Ref. [111] for further discussion).

There were five major questions that needed to be addressed before one could fit and quantify Raman spectra of silicate glasses/melts with confidence.[81] First, what line shapes should be used to fit these Raman spectra: Gaussian, Lorentzian, or mixed Gaussian–Lorentzian? Second, are the FWHM well defined, as observed for crystals, and are the FWHM for all Q species of silicate glasses and melts similar? Third, are all the peaks contributing to the 800–1200 cm^{-1} region due solely to A_1 symmetric stretches from the SiO_4 tetrahedra as in crystals, or are there "additional" peaks? Fourth, are these peaks located at well-defined frequencies? Fifth, and most importantly, if there are "additional" peaks in the 800–1200 cm^{-1} region, what are their origins? In 2015, we re-examined the previously published Raman spectra of alkali silicates[27] to address these questions and show that Raman spectroscopy could become a quantitative technique for obtaining Q species distributions.

First, consider line shapes. The inherent Raman line shape for inorganic glasses is Lorentzian,[112,113] as clearly stated by Efimov[113] (page 100): "*the band shape … unaffected by disorder is known to have a Lorentzian contour*". For crystalline silicate minerals, the Raman peaks are also Lorentzian.[55,114,115] As stated by Rossano and Mysen,[116] disorder in glasses should introduce a Gaussian component to line shapes; however, all binary alkali and alkaline-earth glass Raman spectra considered in the recent literature[79–85] yield > 50% Lorentzian peaks. It is likely that more complex glasses will exhibit a larger Gaussian component, but this remains to be tested.

There were early attempts to consider peak shapes other than Gaussian;[26,50,117] however, most papers, such as Matson's high-quality Raman spectra of alkali silicates,[27] did not fit their spectra or comment on line shapes. Mysen[26,51–54] did fit his spectra, but did not explore alternative line shapes, probably because Lorentzian and Gaussian–Lorentzian fitting programs were not available. Mysen states that "it is also assumed that the individual bands have Gaussian line shape".[26] There was only one publication (in 1984) that strongly indicated that a Lorentzian line shape yields a better fit than a Gaussian line shape for a K silicate glass,[117] but this paper was largely ignored.

Because of the dominance of Gaussian line shapes in the literature, it was initially quite surprising that our new spectra of alkali silicates[79–82] gave consistent peak shapes of high Lorentzian character (e.g. Fig. 7). It is critical to emphasize that we do not "choose" a line shape or make any "assumptions" (as Mysen[26] did above) about the peak shape. A large Lorentzian character is immediately indicated by the "tails" in Fig. 7 on the narrow, intense Q^3 peak. An unconstrained fit, which varies the Lorentzian/Gaussian character as well as the peak position and width, yields the best fit to the spectra.

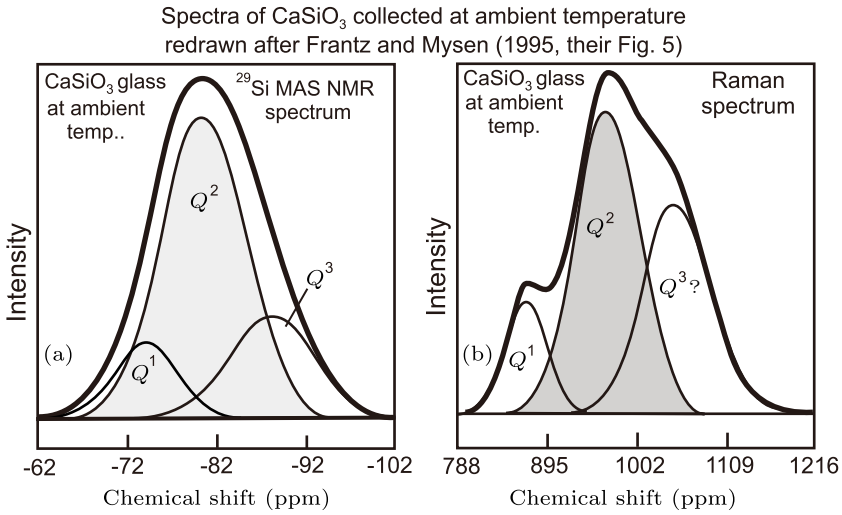


Fig. 6. The ^{29}Si MAS NMR spectrum (left) and Raman spectrum (right) of $CaSiO_3$ glass at ambient temperature, redrawn from Fig. 5 of Ref. [52]. Note the disputed Q^3 assignment in the right-hand peak of the Raman spectrum.

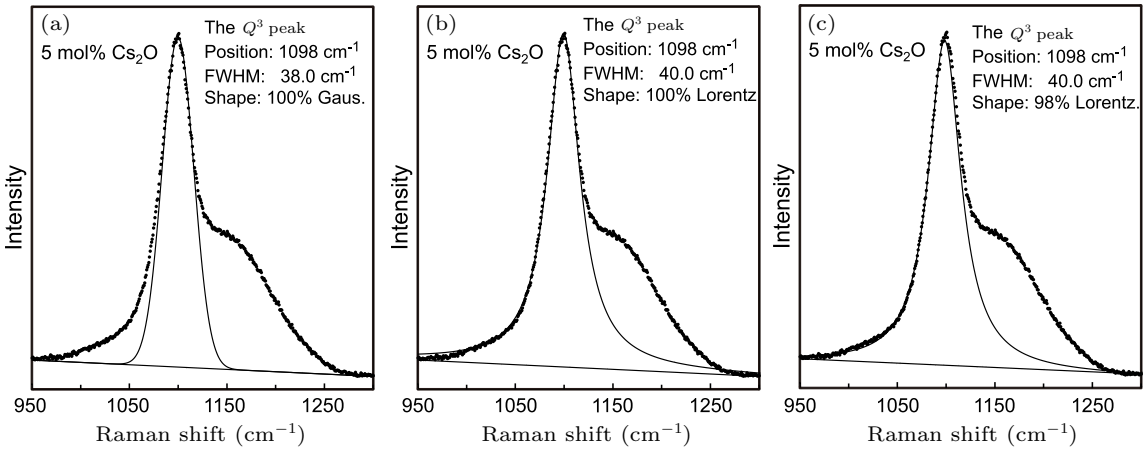


Fig. 7. Different peak shapes used to fit the Q^3 peak in a 5 mol% Cs_2O glass: (a) Gaussian, (b) Lorentzian, and (c) 98% Lorentzian-Gaussian, redrawn from Ref. [81].

There are no constraints on the Q^3 peak parameters (position, width, and %Lorentzian) in this fitting procedure. The Cs and Rb silicate glass spectra are nearly 100% Lorentzian, with 98% Lorentzian giving the best fit for the spectrum of the 5 mol% Cs_2O glass in Fig. 7(c). The Lorentzian "tails" are obvious in these spectra; if a Gaussian were used (Fig. 7(a)), other small peaks would be required to fit the "tails" (e.g., see Fig. 3 of Ref. [76]). As noted above, the Q^2 and Q^3 line shapes in all other alkali and Ba silicate spectra[79–85] are 50–80% Lorentzian. The use of a strong Lorentzian component is especially important where a major central band is flanked by two much weaker bands, such as seen in the ^{29}Si NMR spectrum in Fig. 5(b). The line shape of the large central Q^2 peak can make a significant difference to the area of the small unresolved Q^3 peak (see Subsection 2.5 below).

Second, the linewidths (FWHM) for well-resolved peaks (e.g., the Q^3 peak in Fig. 7(c) or the Q^2 peak in Fig. 8) of many Raman spectra of binary alkaline and alkaline-earth glasses are similar at 40–55 cm^{-1}.[79–83] The Q^1 linewidths, however, are appreciably narrower ($\leq$ 30 cm^{-1}), as evident in spectra of Ba silicates.[84,85] Also, the linewidth of the overall composite Q^3 band is broader than that of the Q^2 band (Fig. 8). The linewidths are quite constant as a function of composition in a given binary system. For example, in the Cs spectra noted above, the Q^3 linewidth varies from 40–55 cm^{-1} over 5–30 mol% Cs_2O.[79–82] In melts, the linewidths are appreciably larger and often approach 100 cm^{-1} (see later in Subsection 2.6).[52,55]

We now address the third problem–the assignment of the peaks. The early Raman studies[23–28] assigned peaks at $\sim$ 850 cm^{-1}, $\sim$ 950 cm^{-1}, and $\sim$ 1100 cm^{-1} to the Q^1, Q^2 and Q^3 species, respectively (Figs. 6–8). As summarized by McMillan,[28,110] these major peaks can be readily assigned to the A_1 symmetric stretches of SiO_4 tetrahedra of those Q species, and recent calculations confirm these assignments.[111] The cross sections for these A_1 stretches for different Q species should be similar.[25,83,118,119] Furukawa's initial calculations[25] indicated that the Q^2 cross section should be $\sim$ 30% larger than the Q^3 cross section; however, two later papers[118,119] gave virtually equal cross

sections for Q^2 and Q^3. Also, it was concluded[81] from a comparison of the ^{29}Si NMR and Raman spectra of a $\sim$ 50 mol% Na_2O glass that the Q^1 cross section was similar to those of Q^2 and Q^3. The Q^4 peak is unusual, because the Q^4 tetrahedron in vitreous SiO_2 does not have an A_1 stretch in this region.[120] However, a detailed analysis of the Q^3 and Q^4 intensities in Cs glasses[80] shows that the Q^4 cross section is not appreciably different from the Q^3 cross section for $\geq$ 30 mol% Cs_2O glasses. For the glasses in this paper ($\geq$ 40 mol% M_2O), the Q^4 abundance is small, as shown by static ^{29}Si NMR for the 40 mol% Na_2O and BaO glasses (2% and 6.7%, respectively[32,84]).

Fourth, the peak maxima for a given Q species are usually similar, as emphasized by McMillan.[28,110] For example, the Q^3 peak maxima in all alkali and alkaline-earth glasses with $\leq$ 40 mol% M_2O are at 1080–1105 cm^{-1};[23–28,79–85,110,111] and for a series of Cs glasses between 5 and 30 mol%,[80] the range is 1095 to 1099 cm^{-1}. In contrast, the Q^2 peak position decreases significantly as the electronegativity (EN) of the cation decreases from Li to Cs (e.g., from 954 cm^{-1} for Li to 928 cm^{-1} for Cs[27,106]). Also, for $\geq$ 45 mol% Na, K and Ba glasses,[76,81,84] the Q^3 peak broadens and shifts to significantly lower energy, as discussed in the next section (Section 2.4) on K glasses.

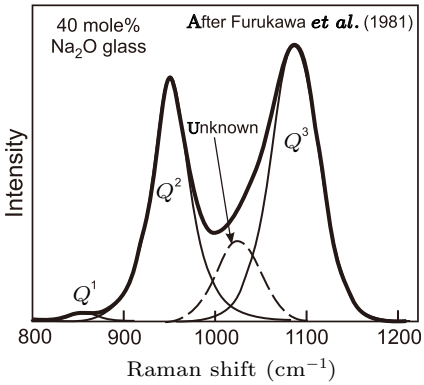


Fig. 8. The redrawn Raman spectrum of a 40 mol% Na_2O glass from Fig. 5 of Ref. [25] (1981), showing the Q^1, Q^2, and Q^3 peaks along with a dashed, unidentified peak at $\sim$ 1028 cm^{-1}. Note that this spectrum is virtually identical to the spectrum in the earliest publication in 1975,[23] and very similar to the spectra decades later in Fig. 9(c).[57,83]

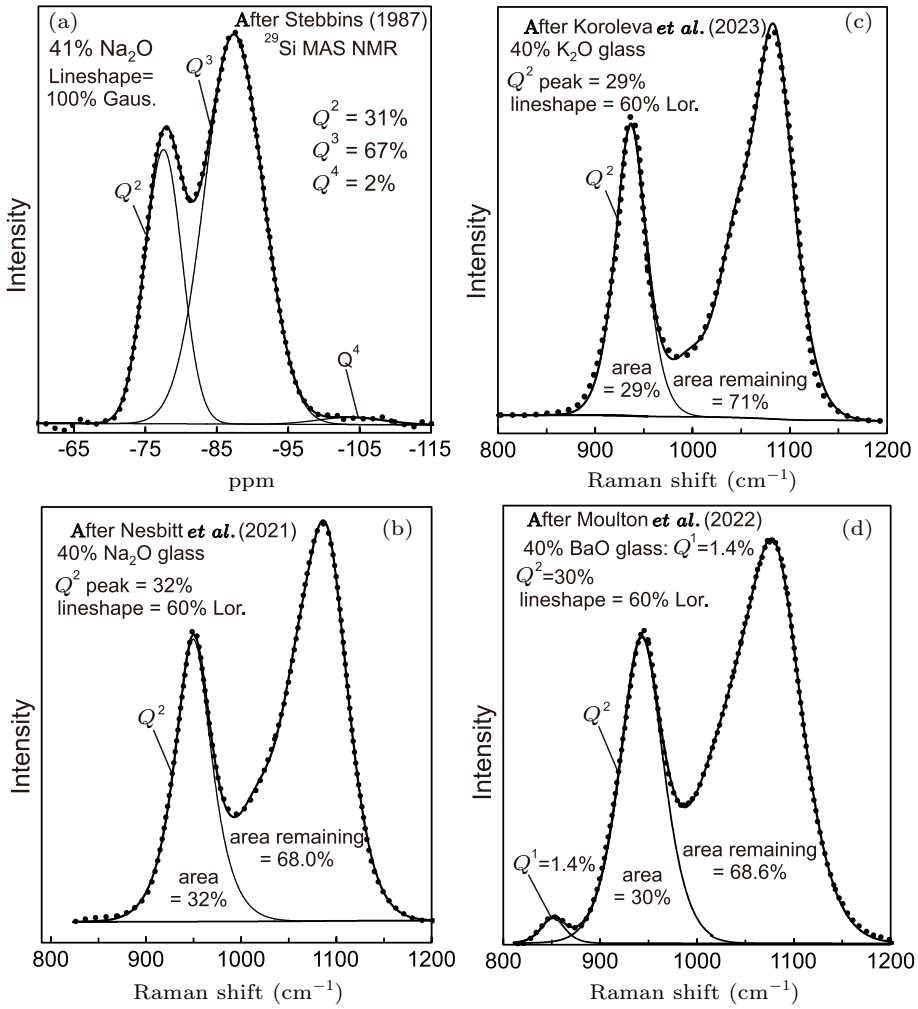


Fig. 9. (a) The fitted ^{29}Si MAS NMR spectrum of the 41 mol% Na_2O glass[32] (the same as in Fig. 4(a)), compared directly with the better resolved Raman spectra of (b) 40 mol% Na_2O,[57,83] (c) digitized 40 mol% K_2O,[76] and (d) the original Raman data of 40 mol% BaO.[84,85] The well-resolved Q_2 peak in all three Raman spectra is best fit by a 60% Lorentzian line shape. Note the very similar intensity of that peak ($\sim$ 30%) in all four spectra.

The fifth problem–the origin of "extra" peaks–is addressed using the ^{29}Si NMR and Raman spectra in Figs. 9 and 10. Figure 9(a) shows the ^{29}Si NMR spectrum of the 41 mol% Na_2O glass again[32] (see also Fig. 5(a)), highlighting the similarity of this NMR spectrum with the three Raman spectra of the 40 mol% Na_2O, 40 mol% K_2O, and 40 mol% BaO glasses (Figs. 9(b)–9(d), respectively). All four spectra consist of two intense peaks, with the peak on the left being less intense and narrower than the peak on the right. Because of the poorer resolution of the ^{29}Si NMR spectrum, it is likely that some of the broadening of the 88 ppm peak in Fig. 9(a) is due to the asymmetric broadening seen on the 1100 cm^{-1} peak in all three Raman spectra (Figs. 9(b)–9(d), see later). Perhaps surprisingly, in all four spectra, the left peak is always $30 \pm 2\%$ of the total intensity of the spectrum (Table 1).

The assignment of the ^{29}Si NMR spectrum in Figs. 5(a) and 9(a) is conclusive:[32,83] the smaller peak on the left arises from Q^2 and the larger peak on the right arises from Q^3. The O mass balance (Eq. (15)) demands that the Q^3 intensity is about double the Q^2 intensity, as seen from the average ^{29}Si NMR values of X_{Q3} and X_{Q2} of 0.68 and 0.29 in Table 1. Note the excellent agreement with the observed Raman intensities of $\sim 70\%$ and $\sim 30\%$. This agreement indicates that the assignment of the Raman spectrum must be analogous: Q^2 at ~ 950 cm^{-1} and the broader asymmetric Q^3 at ~ 1100 cm^{-1}. This mass balance confirms that the broader Q^3 peak in the ^{29}Si NMR spectrum, and the asymmetric high-energy peak in the Raman spectrum, are due solely to the Q^3 species. If the broad 1050 cm^{-1} peak (with about 30% of the area of the total spectrum[83]) is not due to Q^3, e.g., from a "Si–O" peak[51–54] or an SiO_2 peak,[75] then the ratio of Q^3/Q^2 becomes ~ 1.4 instead of ~ 2 required by the O mass balance. If the 1050 cm^{-1} peak arises from a second Q^2 peak,[54,55,76] then the Q^3/Q^2 ratio is ~ 0.7, which is clearly inconsistent with mass-balance considerations.

These O mass balances, along with the similarity of the Q^2 and Q^3 intensities in all four spectra, show conclusively: (1) the asymmetry in the Q^3 Raman peak arises solely from Q^3 species; (2) the Raman cross sections for Q^2 and Q^3 are close to unity in all three Raman spectra; and (3) the Q species distributions in all three Raman spectra are remarkably similar. As initially suggested by McMillan,[110] the Q^3 peak is due to two or more distinct Q^3 environments. We have proposed that the "extra" Q^3 peak(s), shifted by > 60 cm^{-1} from the main peak in Fig. 8, result from at least one Na atom bonded to BO as well as NBO.[81] Our observation of two or more BO peaks in the O 1s XPS spectra of Na and K glasses (Figs. 2 and 3) arises from these M–BO interactions;[20,21] and this result pointed us toward the important role of Na–BO bonding in Raman spectra. When the electropositive Na, K or Ba donates charge to a BO in the SiO_4 tetrahedron, the Si–O Coulombic interaction is reduced, the Si–O force constant decreases, resulting in a lower Q^n Raman frequency of the A_1 symmetric stretch, and a decrease in the O 1s binding energy from BO to NBO.[121,122] The same charge-transfer mechanism is responsible for the decrease in Raman frequencies from Q^3 to Q^1 (~ 250 cm^{-1}) and in O 1s binding energies (~ 2 eV) between NBO and BO when Na forms an NBO via Eq. (3).

The best fits to these four spectra are shown in Fig. 10. There are a few important observations. First, the Q^3 peak in the three Raman spectra (Figs. 10(b)–10(d)) has been fit using three peaks of identical shape (60% Lorentzian for all three spectra) and equal (but not constrained) widths of 55 cm^{-1}, 52 cm^{-1}, and 63 cm^{-1} for Figs. 10(b)–10(d), respectively. These three peaks represent two M–BO interactions on the three BOs in this Q^3 species, e.g., Q^3-0, Q^3-1, and Q^3-2, where 0, 1, and 2 indicate no, one, and two Na–BO bonds, respectively. No additional constraints are used other than peak shape and linewidth equality. Other fits with either two Q^3 peaks[83] or four Q^3 peaks[81] have also been applied successfully. A theoretical study also indicates that a range of different Q-species environments can be used to fit spectra of Na silicate glasses.[123] Second, and most importantly for quantification, the percentage of Q^2 in all three spectra in Figs. 10(b)–10(d) is $30 \pm 2\%$, as in Fig. 9, and the Q^2 and Q^3 fractions are not dependent on the number of Q^3 peaks used in the fit. Third, each M–BO interaction decreases the SiO_4 A_1 symmetric stretch frequency by ~ 40 cm^{-1} [81,83] in all three spectra, consistent with similar electronegativities (EN) for Na, K, and Ba (0.93, 0.823, and 0.89, respectively). Indeed, the Q^3-0, Q^3-1, and Q^3-2 peak positions in all three spectra are similar: 1090 cm^{-1}, 1056 cm^{-1}, and 1015 cm^{-1} for Na (Fig. 10(b)); 1084 cm^{-1}, 1044 cm^{-1}, and 995 cm^{-1} for K (Fig. 10(c)); and 1083 cm^{-1}, 1048 cm^{-1}, and 1013 cm^{-1} for Ba (Fig. 10(d)). The average of these values (1086 cm^{-1}, 1049 cm^{-1}, and 1007 cm^{-1}) will be used in a subsequent discussion (and Fig. 11) of the 40–50 mol% samples when discussing the changes in Raman frequency and linewidth of the Q^3 peak.

The above assignment is now consistent across Na, K, and Ba Raman studies[81,84,85]: the entire asymmetric 1100 cm^{-1} peak arises from Q^3 moieties. A recent independent paper supports this assignment.[78] However, resistance remains,[74,76,124] which is not surprising after 40 years of debate.

The ^{29}Si NMR results from Table 1 (with a new result from our fit to the spectrum in Fig. 5(a), reported in Table 2, second line) all yield FO values between 1 and 3 mol%, and the average of 1.9% likely has an uncertainty of ± 1 mol%. The Q^2 and Q^3 Raman cross sections were obtained by comparing the ^{29}Si NMR abundances (assuming equal cross sections) with the Raman intensities. As shown in Table 1, the

average Q species abundances from the ^{29}Si NMR spectra for Q^1, Q^2, Q^3, and Q^4 for the 40 mol% Na_2O glass are: 0.0%, 28.8%, 68.8%, and 2.4%, respectively. The Raman spectral intensities (taking 2.0% out of the Q^3 intensity for Q^4 based on the static ^{29}Si NMR spectrum) are: 0.6%, 32.2%, 65.2%, and 2.0%, respectively (Table 2). Considering that the spectral intensity of a Q^n species (I_{Q^n}) is the product of its cross section (σ_{Q^n}) and mole fraction (X_{Q^n})

$$I_{Q^n} = \sigma_{Q^n} X_{Q^n}. \tag{18}$$

The σ_{Q3} is then 0.95 (65.2/68.8), and the σ_{Q2} is 1.12 (32.2/28.8). Similar cross sections for Q^n (n = 1–3) are expected from previous experimental and theoretical results.[81,115,116]

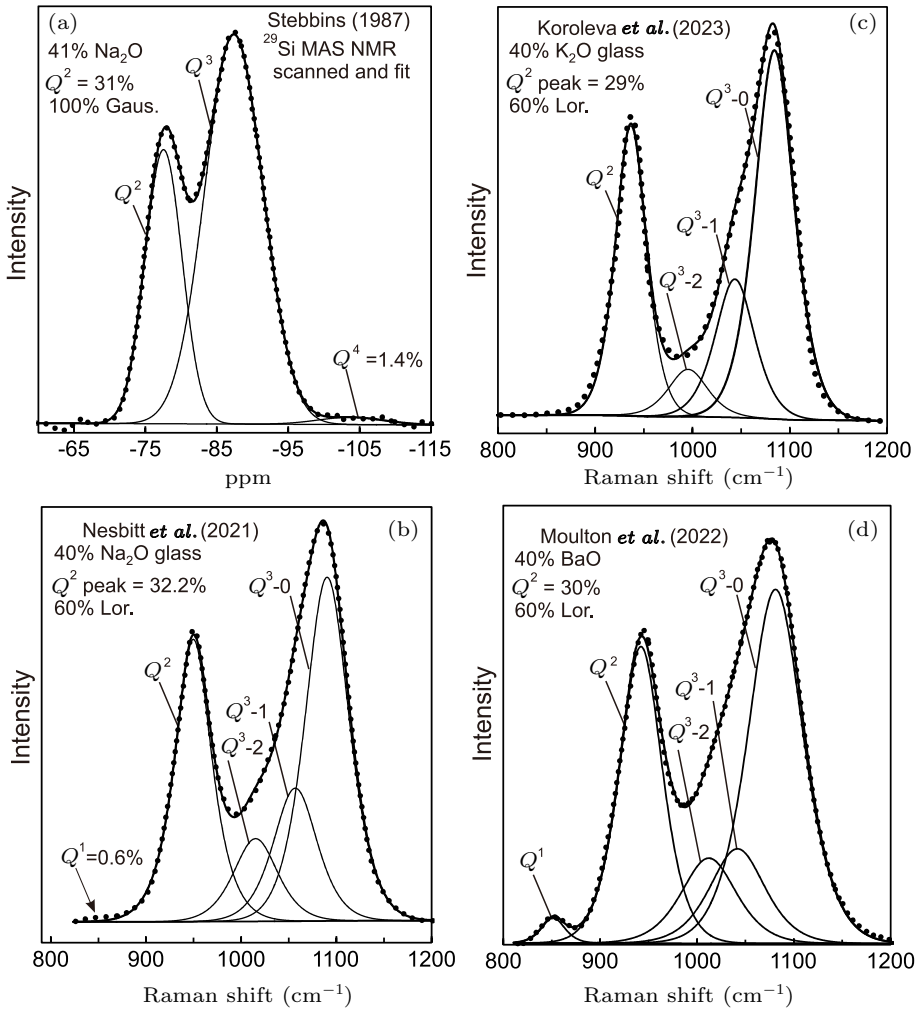


Fig. 10. (a) The fitted NMR spectrum is identical to Fig. 9(a) but is included for easy comparison with the complete fits to the three Raman spectra in Fig. 9. Note the nearly constant intensity of the Q^2 peak ($\sim$ 30% in all cases), and the three Q^3 peaks of equal width used to account for the asymmetry of the Q^3 band.

To quantify other Raman spectra of silicate glasses containing different amounts of Na, or containing other elements such as K and Ba, these cross sections would need to apply universally. Is this possible? Considering that the Ba and K spectra are very similar to the Na spectrum (e.g., uncorrected % Q^1, Q^2, and Q^3 for the 40 mol% BaO spectrum in Table 2 are 1.4%, 29.5%, and 69.1%, respectively[84]), it is worth exploring this possibility. Our independent fit of the 40 mol% Ba spectrum (Fig. 10(d)) gives Q species distributions (1.2%, 30.2%, and 68.6%, Table 2) in excellent agreement with Moulton's values.[84] Moulton[84,85] derived cross sections from his own ^{29}Si NMR spectra of Ba silicate glasses and compared them with the above values for the 40 mol% Na_2O spectrum. He obtained Q^3 and Q^2 cross sections close to 1 for Ba glasses containing $\sim$ 35 mol% BaO, but the difference between σ_{Q3} and σ_{Q2} became larger for the 40 mol% (1.21 and 0.81) and 45 mol% (1.40 and 0.79) BaO glasses. Note that $\sigma_{Q3} > \sigma_{Q2}$ for all Ba glasses, whereas $\sigma_{Q3} < \sigma_{Q2}$ for the 40 mol% Na_2O glass. Most of this difference is likely due to the poor resolution of the ^{29}Si NMR spectra of Ba glasses. These ^{29}Si NMR spectra, and indeed all ^{29}Si NMR spectra of alkaline-earth silicates, have no defining features (e.g., see Fig. 6(a) for the spectrum of $CaSiO_3$ glass). As emphasized in Subsection 1.1 and Ref. [68], it is not possible to obtain quantitative Q species distributions from an unconstrained three-peak fit to spectra with no defining spectral features. All such fits to the ^{29}Si NMR

spectra in the literature have effectively been constrained to Q species distributions that yield FO = 0 (e.g., Table 2). We suggest that it would be better to use equal Raman cross sections for Q^1, Q^2, and Q^3 species and the Q^4 abundance from static ^{29}Si NMR spectra. With this approach, FO = 2.2% for the 40 mol% BaO glass (Fig. 10(d), Table 2). Using the cross sections from the 40 mol% Na_2O spectrum, FO = 2.9% (Table 2). These FO values are consistent with other FO values obtained for alkaline-earth glasses noted earlier (1–2.6 mol%)[69] from other spectra and MD calculations. This promising result indicates that cross sections very close to unity are appropriate for alkali and alkaline-earth glasses.

Now we turn to the quantification of the Raman spectrum of 40 mol% K_2O glass (Fig. 10(c), Table 2). The fit in Fig. 10(c) is remarkably similar to the fit to the Na spectrum in Fig. 10(b), including the three-peak fit to the Q^3 envelope. The 29 mol% Q^2 species is substantially lower than the Q^2 value for the 40 mol% Na_2O fit (31 mol%), indicating greater polymerization (i.e., more FO) in K than in Na glasses. This result is consistent with the O 1s XPS results in Figs. 2 and 3. Using equal cross sections, FO for the K glass (1.2%) is larger than for the Na glass (0.6%). With $\sigma_{Q3} = 0.95$ and $\sigma_{Q2} = 1.12$, the FO of the 40 mol% K_2O glass increases to 1.8 mol%. Note that we also list the abundances from ^{29}Si NMR, but Maekawa does not show his fit for this glass,[41] and Malfait's spectra of 38.5 and 42.9 mol% K_2O glasses[46] have poor resolution and cannot be used to standardize the Raman spectra. Note again that the ^{29}Si NMR Q values yield an FO of 0. Malfait[46] demonstrates one of the "adjustment" techniques that had to be applied to such unresolved spectra.[46,67] Their initial fits yielded negative FO values, which they recognized as physically impossible. They then "adjusted" the numbers in unspecified ways to enforce FO = 0. Some of these adjustments were large.[68]

Table 2. % FO in silicate glasses and melts.

Glass/Melt	Technique	Q^4 (%)	Q^3 (%)	Q^2 (%)	Q^1 (%)	FO (%)	Ref.
40/41 mol%Na (G)	NMR[a]	2.4	68.8	28.8	0.0	1.8[b]	[83], Table 1
41 mol% Na (G)	NMR[b]	1.4	68.0	30.6		2.0	Fig. 10(a)
40 mol% Na(G)	Raman[c]	2.0	65.2	32.2		0.6	Fig. 10(b)
40 mol% Ba (G)	Raman[d]		69.1	29.5	1.4		[84], Fig. 10(d)
	Raman[e]		68.6	30.2	1.2		
	Raman[f]	6.7	65.7	26.2	1.4	2.2	
	Raman[g]	6.7	68.5	22.4	1.4	2.9	
	NMR	7	55	33	5	0	
40 mol% K (G)	Raman[h]	1.6[i]	69.3	29.1		1.2	[76], Fig. 10(c)
Figs. 9(c) and 11(a)	Raman[g]	1.6	72.5	25.9		1.8	
	NMR		67	32	1	0	[41]
50 mol% K (G)	NMR	9	47	37	7	9.7	[41]
Figs. 11(a) and 11(c)	NMR[j]		56	37	7	8.2	[41]
	Raman[h]		47.1	51.5	1.4	7.4	[76], Fig. 11
	Raman[g]		51.2	47.4	1.4	8.5	
50 mol% Na(G)	Raman		30	64	6	4	[81]
Figs. 11(c) and 5(b)	NMR		16	70	13 + 1	~0	[41,63]
	NMR[k]		28.5	66.0	13 + 1	0.6	[64]
50 mol% Na(M)	Raman[h]		35	58	7	4.7	[55], Fig. 12(a)
50 mol% Li (M)	Raman[h]		35	60	5	5.0	[55], Fig. 12(b)
50 mol% Ca	Raman[h]		30	60	10	3.3	[52], Fig. 12(c)

(a) Average Q % from Table 1. (b) Our fit to the 41% Na_2O spectrum from Ref. [32]. (c) Uncorrected raw data with equal cross sections and $Q^4 = 2\%$ from static ^{29}Si NMR. Using Raman cross sections $\sigma_{Q3}(1.12)$ and $\sigma_{Q2}(0.95)$ from NMR yields FO = 1.8%.
(d) Uncorrected raw data.[84] (e) Our fit to the same spectrum. (f) Normalized data for the 6.7% Q^4 from static NMR using equal cross sections. (g) Same data using $\sigma_{Q3}(1.12)$ and $\sigma_{Q2}(0.95)$. (h) Assuming equal cross sections. (i) Q^4 from extrapolation of static ^{29}Si NMR of 33.4 and 36.4 mol% Na_2O samples.[41] (j) Added Q^4 to Q^3. (k) Using the measured mol% Na_2O of 47.6%.[64]

Several important conclusions follow directly from our analysis of Figs. 9 and 10, along with Tables 1 and 2. First, the best-resolved ^{29}Si MAS NMR spectrum for the 41 mol% Na_2O glass, and three other such studies on 40 mol% Na_2O glasses (Table 1),[32] provide strong evidence for ~ 2 mol% FO in these glasses.[32] As correctly stated by Stebbins,[63] these FO values are quite sensitive to chemical composition (e.g., a decrease in Na_2O content of 1% causes a decrease in FO of ~ 1%) and to small amounts of Q^1 and Q^4 species; however, the overall uncertainty is less than ±1 mol%, especially considering that there are four independent measurements quoted in Table 1[32,41,42,64] along with our independent fit in Fig. 9(a). Second, the quantitative comparison of the ^{29}Si NMR and Raman spectra of the 40/41 mol% Na_2O samples shows that the Raman spectrum can be assigned to a narrow Q^2 peak and a broader asymmetric Q^3 peak. Third, the Raman spectra can be fitted without constraining intensities, resulting in Raman cross sections that are close to unity.

Fourth, for the three 40 mol% samples, the Q^3 peak is composed of three components, each separated by about 40 cm^{-1}, which are attributed to M–BO interactions that decrease the Q^3 Raman frequency. Fifth, the remarkable similarity of the Na, Ba, and K spectra shows that there is a comparable amount of FO ($\sim$ 2 mol%) in the three glasses. Sixth, the similar amounts of FO in these alkali and alkaline-earth glasses indicate that the thermodynamic treatment of Eq. (1) based on crystalline phases[61–63] cannot be applied to homogeneous solid solutions, as pointed out by Fraser[125,126] and Nesbitt.[64] Moreover, the cation field-strength argument used by Stebbins[61–63] does not predict the degree of polymerization: low-field alkali cations produce FO comparable to that in alkaline-earth glasses.

2.4. Raman results for 50 mol% K_2O glass with reinterpretation of the ^{29}Si NMR spectrum showing $\geq$ 7 mol% FO

There is strong evidence for FO in the 40 mol% Na_2O glass as indicated by both ^{29}Si NMR and Raman spectra. In both cases, the Q^3 abundance is greater (i.e., the glass is more polymerized) than expected if only disproportionation reactions occurred. Moreover, the similarity of the Raman spectra of 40 mol% Na_2O, K_2O, and BaO glasses indicates $\sim$ 2 mol% FO in all three systems. Even stronger evidence for FO in potassic glasses is provided by re-analysis of the classic ^{29}Si NMR spectrum of 50 mol% K_2O glass (Fig. 11(a)) from 1991.[41] The original spectrum was misassigned,[41] it was misassigned again in 2007,[46] and it remained misassigned in 2020.[63] As now shown, with reassignment, the 50% K_2O glass contains 7–9 mol% FO, which is consistent with the O 1s XPS results in Fig. 3.

Maekawa *et al.*[41] noted that the 50% K_2O spectrum (Fig. 11(a)) was different from other metasilicate ^{29}Si NMR spectra in that it contained two intense bands. The 50% Na_2O glass spectrum (Fig. 5(b)), as well as all previously published ^{29}Si NMR spectra of alkali and alkaline-earth silicates, showed no indication of two resolved peaks arising from a single Q species, and the assignment of the 50 mol% K_2O spectrum was therefore not straightforward. By Ockham's razor, the simplest approach would be to assign the four spectral bands to four different Q species: Q^1, Q^2, Q^3, and Q^4 at 70.8, 76.2, 81.7, and 89.0 ppm, respectively, as had been done for earlier NMR spectra. Maekawa *et al.*[41] considered this possibility, but it leads to $Q^3 \gg Q^1$, with NBO/Si = 1.44, which was inconsistent with the disproportionation reaction (i.e., $2Q^2 \Leftrightarrow Q^1 + Q^3$). By "conventional wisdom," the assignment was therefore regarded as incorrect (and not publishable).

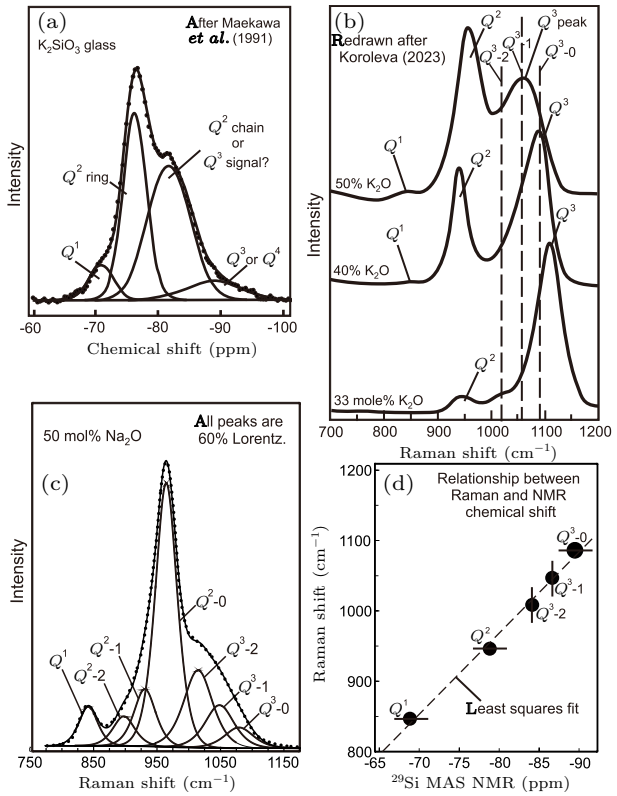


Fig. 11. (a) The ^{29}Si NMR spectrum of the 50 mol% K_2O glass redrawn from Ref. [41], including the original fit.[41] (b) The Raman spectra of 33, 40, and 50 mol% K_2O glasses redrawn from Fig. 1 in Ref. [76]. (c) The Raman spectrum of Na_2SiO_3 (Fig. 9 in Ref. [52]) with three Q^2 and three Q^3 peaks redrawn from Ref. [81]. The dashed lines represent the approximate positions of the Q^3_0, Q^3_1, and Q^3_2 peaks. Note the similar relative heights and widths of the Q^2 and Q^3 bands in both the ^{29}Si NMR spectrum (a) and the Raman spectrum of K_2SiO_3 glass (top of (b)). (d) Plot of Raman shift versus ^{29}Si NMR peak position for the Q^3_0, Q^2, and Q^1 Raman species from Fig. 10(b), along with a visually fitted straight line through the three data points. The Q^3_1 and Q^3_2 Raman positions from Fig. 10 are plotted on the same line to show that the expected Q^3_2 position (see Fig. 10(b)) is < 85 ppm.

The prevailing view required $Q^1 = Q^3$ and NBO/Si = 2.0 for all metasilicate glasses. Maekawa *et al.*[41] thus adopted a more complex interpretation, stating that: "If we assume instead that two types of the Q^2 species are present in the potassium silicate glasses and the two (intense) peaks at $\sim$ 82 ppm and $\sim$ 76 ppm (Fig. 11(a)) are both assigned to Q^2 species, the NBO/Si ratio satisfies the stoichiometric value" (2.0). He acknowledged that there was no direct evidence for two Q^2 species in alkali glasses but suggested that Q^2 species in chain and ring configurations observed in potassium silicate aqueous solutions could give rise to two Q^2 signals. There was, however, no evidence for chains in silicate glasses, as noted in Henderson's 2005 review (Ref. [17] in 1942), and there is still no evidence in 2025. Despite this lack of evidence, subsequent ^{29}Si NMR and Raman studies[46,58,59] adopted the "two Q^2 peak hypothesis," including Stebbins' review in 2020[63] and Koroleva's work in 2023.[76] Because of the high reactivity of this glass, it is important to note that later ^{29}Si NMR spectra of 50 mol% K_2O glass[46,63] are very similar to the Maekawa spectrum[41] shown in Fig. 4(b), strongly suggest-

ing that the composition is close to the nominal 50 mol%, and that no significant decomposition occurred in these studies.

There is now strong Raman evidence supporting a simple "one peak per Q species" assignment. It comes from the latest Raman spectra of 30–50 mol% K_2O glasses shown in Fig. 11(b).[76] Each Q species exhibits a single resolved band in these spectra. Specifically, Q^1 appears at ~ 850 cm^{-1}, Q^2 at ~ 950 cm^{-1}, and Q^3 at 1070–1100 cm^{-1}. The Q^3 band is broadest for the 50% K_2O glass (Fig. 11(b)), but importantly, only one Q^2 band is observed. The assignments for the 50 mol% K_2O glass spectrum (Fig. 11(b)) correlate closely with the ^{29}Si NMR spectrum (Fig. 11(a)): both exhibit a weak Q^1 feature at low ppm/frequency, an intense, relatively narrow Q^2 peak at intermediate ppm/frequency, and a broad, intense Q^3 peak at higher ppm/frequency. If two distinct Q^2 contributions were present in potassic glasses, they would have been resolved in the higher-resolution Raman spectrum of the 50 mol% K_2O glass. The Malfait *et al.*[58] spectra for 39.1–49.4 mol% K_2O glasses (their Fig. 6), as well as the 40 mol% Na, K, and Ba spectra (Figs. 10(b)–10(d)), show the same sequence of bands. The correlation of peak assignments between Raman and ^{29}Si NMR spectra strongly indicates that the broad intense peak in the ^{29}Si NMR spectrum (centered at ~ 82 ppm) corresponds to a Q^3 band, while the weak feature centered at ~ 90 ppm corresponds to a Q^4 band. Ockham's razor therefore leads to a simpler and more consistent interpretation of the K silicate ^{29}Si NMR spectrum.

In both the ^{29}Si NMR and Raman spectra, the increase in broadening and the shifting to lower energy of the Q^3 band from 30–50 mol% K_2O is readily explained using the expected increase in K-BO interactions with increasing K content. Consider this K-BO effect on the Raman spectrum first. As outlined earlier, each K-BO interaction decreases the SiO_4 A_1 symmetric stretch frequency. As already shown for the three 40 mol% Raman spectra in Figs. 9 and 10, the three Q^3 peaks (Q^3-0, Q^3-1 and Q^3-2) are at ~ 1090 cm^{-1}, ~ 1050 cm^{-1} and ~ 1010 cm^{-1} respectively (also see Figs. 11(b) and 11(c)). The Q^3-1 and Q^3-2 peaks should become more intense with addition of K from 40 mol% to 50 mol% (Fig. 11(b)). The increase in Q^3-1 and Q^3-2 peak intensities has to: (1) shift the Q^3 peak maximum to lower energy and (2) broaden the overall peak, as observed. This effect is even more noticeable in the Raman spectrum of the 50 mol% Na_2O glass (Fig. 11(c)), published by several groups,[23,52,55,127] where the overall Q^3 maximum is close to 1000 cm^{-1}, and Q^3-2 is the most intense Q^3 peak.

Now consider, apparently for the first time, the K-BO effect on the chemical shifts and peak widths in the ^{29}Si NMR spectra. Nearly all the ^{29}Si NMR studies of Na and K glasses (e.g. Refs. [32,41,63,64]) show that the full-width at half-maximum (FWHM) increases markedly from Q^1 (≤ 5 ppm) to Q^2 (6–7 ppm) to Q^3 (10–11 ppm), and these linewidths are independent of the magnetic field strength (4.7 T to 14 T) used to obtain these spectra (as noted earlier). Note that the Raman linewidths also increase similarly,[81–85] although it is more difficult to obtain a quantitative overall Q^3 linewidth from the asymmetric Q^3 peaks in Figs. 9 and 10. For example, the Q^1 and Q^3 Raman linewidths for the 40 and 50 mol% Na_2O and K_2O glasses are ~ 40 cm^{-1} and > 70 cm^{-1} respectively (Figs. 10 and 11[81]). Only Maekawa[41] has mentioned this large variation in the Q species NMR linewidths, and he attributed the large difference between Q^1 and Q^3 to a larger distribution in 'bridging angle, bond length or third neighbor environments' as n increases from Q^1 to Q^3. Our K-BO mechanism mentioned above for Raman and O 1s spectra can now explain the broadening and shifting of the Q^3 peak as K increases.

In Fig. 11(d), we show the strong correlation between the Raman shift and ^{29}Si NMR shifts for Q^1, Q^2 and Q^3. The ^{29}Si NMR Q^2 and Q^3 chemical shifts were obtained by averaging values for the 33.3 mol% and 36.4 mol% Na_2O and K_2O glasses;[41] and the Q^1 chemical shift is the average of the chemical shift from the 50 mol% glasses.[41] Results from other NMR studies are in good agreement.[63,64] The Raman frequencies (Q^3-0, Q^2 and Q^1) are derived from averaging the frequencies from the three fits in Figs. 10(b)–10(d). The range of Raman and ^{29}Si NMR shifts are indicated by the bars. Clearly, when the NMR shift becomes more negative, the Raman shift increases; and the trend is close to linear between all five Q species. From the average Q^3-1 and Q^3-2 Raman shifts (1049 cm^{-1} and 1008 cm^{-1}), we can then predict that the ^{29}Si NMR chemical shift decreases substantially from 89.5 ppm (Q^3-0) to ~ 86.5 ppm (Q^3-1) to ~ 83.5 ppm (Q^3-2) as shown in Fig. 11(d). When Q^3-2 is the most intense peak at ~ 1000 cm^{-1} in the Raman spectrum (as indicated in Fig. 11(c) for the 50 mol% Na_2O spectrum), the NMR peak should shift by ~ 6 ppm to ~ 84 ppm as shown more clearly by the resolved peak in the K_2O NMR spectrum at 82 ppm (Fig. 11(a)). Thus, a shift in the Raman Q^3 peak (from Q^3-0 to Q^3-2) by ~ 80 cm^{-1} leads to an NMR shift of ~ 6 ppm. This shift to lower frequency in the Raman spectra (Fig. 11(b)), and the broadening from larger amounts of Q^3-1 and Q^3-2, should have similar effects on the ^{29}Si NMR spectra. This expected shift by ~ 6 ppm in the Q^3 peak is critically important for the assignment of both the 50 mol% K_2O spectrum and the 50 mol% Na_2O spectrum in section 2.6 below. There is no longer any need for a new Q^2 peak as postulated by Maekawa[41] and Malfait[67]: their new Q^2 peak is indeed our Q^3-2 peak broadened by Q^3-1 and Q^3-0. This confirms our previous assignment in 2015[68] and strongly suggests that our plot of ^{29}Si NMR chemical shifts for the 50 mol% alkali silicate glasses (Fig. 3 in Ref. [68]) is the meaningful chemical

shift trend. The trend is no longer "inconsistent with known chemical shift trends".[63,67]

A few theoretical comments on the trends of ^{29}Si NMR chemical shifts, and the reasons for the correlation in Fig. 11(d), are warranted. Obviously, the ^{29}Si peak shifts to smaller negative ppm with increase in electron density on the Si from the increase in Na/K content[121] on going from Q^3 to Q^2. For the 40 mol% Na_2O glass (Figs. 4(a), 9(a) and 10(a)), the Q^3 and Q^2 positions are −88 ppm and −77 ppm respectively. As outlined by Maekawa[41] and Tossell,[128] the ^{29}Si chemical shift shielding constant (σ) consists of three terms, with the local paramagnetic term, σ^{para}, dominating. It can be expressed as

$$\sigma^{\text{para}} = (C\boldsymbol{Q}\langle r^{-3}\rangle)/\Delta E, \tag{19}$$

where C is a constant, $\boldsymbol{Q}$ is the electron density on the Si, $\langle r^{-3}\rangle$ is the expectation value of r^{-3} for valence Si 3p electrons, and ΔE is the average excitation energy from highest occupied molecular orbital (HOMO) to lowest unoccupied molecular orbital (LUMO). The $\boldsymbol{Q}$ and ΔE terms dominate. With the addition of electron density to the SiO_4 tetrahedra from additional Na or K via NBO and/or BO bonds, the $\boldsymbol{Q}$ and ΔE terms reinforce each other; $\boldsymbol{Q}$ increases while ΔE decreases.[121,129,130] Changes in the charge and electron density on the Si from Na and K bonding to the SiO_4 tetrahedra should have a similar effect on the ^{29}Si NMR as has already been discussed for O 1s XPS and Raman spectra. We propose that this change in electron density is the major factor for the NMR chemical shift trend, and a strong contributor to the increase in NMR linewidths from Q^1 to Q^3. Additional theoretical and experimental studies are now required.

From the above assignment of the Raman spectrum to Q^3, and the similarities between the Raman and ^{29}Si NMR spectra, the ^{29}Si NMR spectrum of the 50 mol% K_2O glass must be assigned as suggested by Ockham's razor: one peak per Q species. Without calculating the FO content, it is immediately obvious that $Q^3 \gg Q^1$ and there is a large FO present. This FO has been calculated in four different ways in Table 2. The first FO content from the quoted ^{29}Si NMR intensities[41] is 9.7%. To show the sensitivity of the FO to a change in the assignment, by including the small broad Q^4 peak as Q^3, we obtain 8.2 mol%. From our preliminary fit to the Raman spectrum using equal cross sections, one obtains 7.4%; and by using the Q cross sections from the 40 mol% Na_2O spectrum,[83] 8.5 mol% is obtained. The FO is 7–10 mol%. These values are in good agreement with those predicted by the O 1s results (see Fig. 4). Polymerization is important as reflected in the NBO/Si of ∼ 1.5 (1.44 given initially[41]). Further studies of 40–50 mol% K glasses are required to better quantify the FO content. Unfortunately, the literature ^{29}Si NMR spectra for the 35–50 mol% K_2O samples are very poorly resolved.[67,68]

Obviously, the above results (and the O 1s XPS results in Figs. 3 and 4) show that FO is larger for K glasses than Na glasses of the same composition because of greater polymerization of K glasses. There is additional spectroscopic evidence which supports this conclusion. In the very first 1975 Raman spectra of K and Na silicate glasses (Figs. 2, 3 and 4 in Ref. [23]), it is obvious that the three glasses between 33.3 mol% and 40 mol% M_2O display a Q^2 peak in the K spectrum that is substantially smaller than Q^2 in the Na spectrum. Even for 20 and 25 mol% $(K_x, Na_{1-x})_2O$ (x =0–1) silicate glasses, recent Raman spectra[131] showed that K glasses are more polymerized than the comparable Na glasses, as indicated by the O 1s XPS spectra in Figs. 3 and 4. All these spectra show small peaks due to Q^2, but the K glasses have very noticeable smaller Q^2 than the comparable Na glasses.

2.5. The ^{29}Si NMR spectrum of 50 mol% Na_2O glass: Poor resolution and "adjustments"

In 2020, Stebbins published the ^{29}Si NMR spectra of a number of glasses with ∼ 50 mol% Na_2O and K_2O,[63] all of which were similar to the original spectra published by Maekawa in 1991[41] (Figs. 5(a) and 11(a) respectively, with Maekawa's fits). He concluded that the FO content in both cases was "below detection limits of about 0.5 to 1 mol% FO". There are three serious problems with his study.

First, and most importantly, the resolution of the weak Q^3 shoulder in the ^{29}Si NMR spectrum of 50 mol% Na_2O (Figs. 1 and 5(b)) is not sufficient to obtain an objective estimate of the Q^3 intensity and FO content (see Subsection 1.2). Stebbins emphasizes the problems by using adjustments such as unreported Lorentzian character for the central Q^2 peak to account for the Q^2 "tails",[63] and an extra Q^2 peak (of "no structural significance"[63]). Both of these "adjustments" decrease the Q^3 intensity to give the desired result of FO = 0. Maekawa's fit in Fig. 5(b) has similar problems. The Q^2 peak maximum in his fit reaches the top of the experimental spectrum, and this is not possible with an overlapping Q^3 peak as shown in Fig. 1. Moreover, the three-peak fits from both Stebbins and Maekawa are very similar to the fit in Fig. 1(e), which has the highest RMS value.

Second, his previous ^{29}Si NMR study of the 41 mol% Na_2O sample (see above) yielded 2.8 mol% FO (Table 1) from his own data! The equilibrium considerations from Eq. (3) show that the 50 mol% sample should have about twice the FO as the 40 mol% sample (Fig. 3). Either one study or the other is incorrect! The resolution of Q^2 and Q^3 peaks in the 50 mol% spectrum is poorer than in the 40 mol% spectrum and, as shown above in Subsection 1.1, the 50 mol% spectrum cannot be fit objectively to obtain a reliable Q^3 amount. In contrast, we have already shown that the 40 mol% spectrum can be fit without constraints to give a reliable Q^3 content. The 40 mol% spectrum is far more likely to be correct.

Third, the Raman spectrum of 50 mol% Na_2O glass (Fig. 11(c)) was ignored. This spectrum has been duplicated by at least five groups,[23,52,55,81,127] with the first published in 1975[23] and the latest in 2013.[127] These Raman spectra all show the same major features as the ^{29}Si NMR spectrum — a weak narrow Q^1 peak, a narrow intense Q^2 peak and a very broad unresolved Q^3 envelope. As always, the Raman spectrum is better resolved than the ^{29}Si NMR spectrum and fits to the Raman spectrum (Fig. 11(c))[81] gives FO = 4 mol% (Table 2) assuming equal cross sections. If the chemical composition is only 48 mol% Na_2O (unlikely for all five studies), FO would be ~ 2 mol%. Note also that the Q^3 envelope in the 50 mol% Na_2O Raman spectrum (Fig. 11(c)) is very broad and shifted to lower frequency, as for the 50 mol% K_2O spectrum in Fig. 11(b). Three peaks of equal width (with no position or intensity constraints) give positions of 1079, 1049 and 1015 cm^{-1} as shown by dashed lines on Fig. 11(b). It is perhaps surprising that these two peak positions are so close to those in the 40 mol% spectrum Fig. 10(b), namely 1080, 1050 and 1010 cm^{-1}. This agreement gives more credence to the concept that each of these three Q^3-0, -1 and -2 species can be represented by a well-defined peak.

2.6. The Raman spectra of 50 mol% melts

Several excellent Raman spectra of silicate melts have been published, and three of these spectra of 50 mol% Na_2O, Li_2O and CaO are shown in Figs. 12(a)–12(c).[52,55] Both the spectra and their reasonable fits are taken directly from the two publications.[52,55] All of these spectra yield much broader lines and poorer resolution than for the glasses, as expected from the systematic increase in linewidths as the temperature increases (e.g. see Fig. 7 in Ref. [81]). The three spectra are qualitatively similar with two shoulders (at ~ 850 cm^{-1} and ~ 1050 cm^{-1}) on either side of a strong central peak at ~ 950 cm^{-1}. Using our previous analysis of glass spectra, the peaks/shoulders can be readily assigned to Q^1 (weak shoulder at ~ 850 cm^{-1}), Q^2 (strong peak at ~ 950 cm^{-1}) and Q^3 (strong shoulder at ~ 1050 cm^{-1}). Obviously, $Q^3 \gg Q^1$ with this assignment, indicating significant polymerization and non-zero mol% FO for melts with alkali and alkaline earth cations. In the previous papers,[52,55] the ~ 1050 cm^{-1} peak was not assigned to the expected Q^3 peak,[52,55] mostly because "conventional wisdom" demanded that Q^3 had to be equal to Q^1 to obtain FO = 0 (Eq. (7b)). For example, the 1050 cm^{-1} peak in Fig. 12(c) was assigned to a Si-O^0 bridging oxygen stretching frequency from all Q species.[52] This assignment is now known to be incorrect.[111,120]

Quantification of these poorly resolved spectra is difficult, as emphasized in Subsection 1.1. Different linewidths and lineshapes will substantially affect the Q species estimates. But in this case, it is obvious (much more obvious than for Fig. 1) that $Q^3 \gg Q^1$, indicating non-zero mol% FO in all cases. The spectra were fit in the original publications[52,55] to three or four peaks as shown in Fig. 12. The "extra" smaller peak at ~ 1000 cm^{-1} can be readily assigned to our Q^3-1, as in Figs. 9 and 10 for the silicate glasses. The Q species abundances (Fig. 12, Table 2) are taken from Table 1 in Ref. [52] for $CaSiO_3$ (Fig. 12(c)), and from our equivalent fits to Figs. 12(a) and 12(b) for Na_2SiO_3 and Li_2SiO_3. For a preliminary semi-quantitative estimate of FO in these three melts, we use the Q abundances in Fig. 12 and Table 2. In all cases, $Q^3 \geq 3Q^1$. FO contents of 3.3–5.0 mol% are obtained (Table 2), comparable to the FO of 4 mol% for the 50 mol% Na_2O glass in Fig. 11(c) (Table 2). Note again that the FO abundances for the alkali cations Na and Li are comparable to, or larger than, the FO for the Ca melt. This is one more indication that both Stebbins' thermodynamic treatment based on crystals, and the field strengths of cations,[61–63] are not relevant to the amount of FO in silicate solid solutions.[125,126]

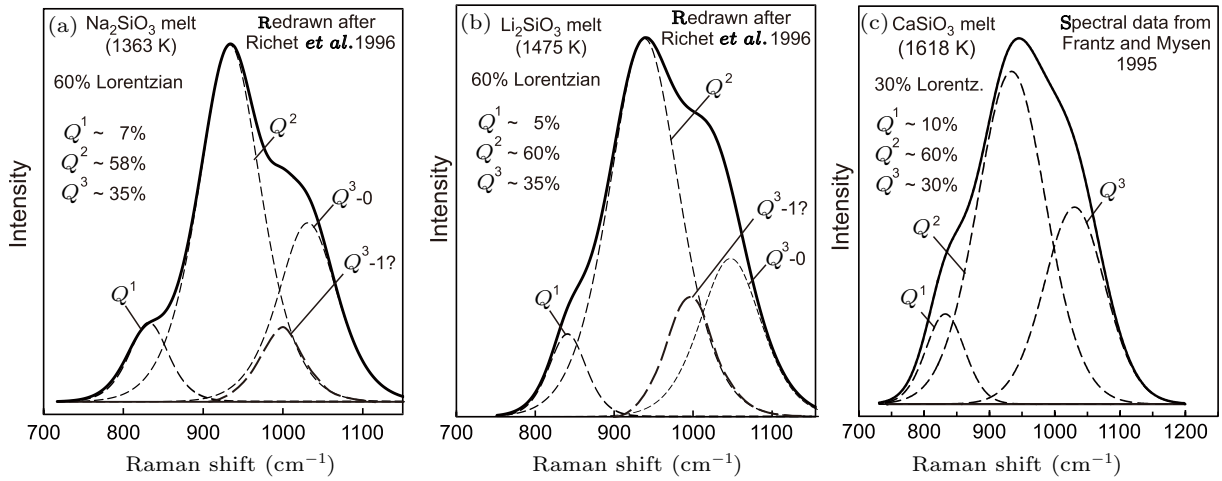


Fig. 12. The Raman spectra (and published fits) of metasilicate silicate melts of (a) Na_2SiO_3 and (b) Li_2SiO_3 (Fig. 12 from Ref. [55]), and (c) $CaSiO_3$ (Fig. 4(c3) from Ref. [52]). The Q^3 peak(s) were not assigned in the previous publications, because Q^3 was assumed not to be larger than Q^1 from the "conventional wisdom" of disproportionation.

2.7. MD simulations on Na_4SiO_4: Methods and FO

Previous simulations of Na-silicate and Mg-silicate glasses and melts[11,101,132,133] indicate the presence of FO. For example, Na_2SiO_3 glass at 300 K[11] yielded 0.47 mol% FO, whereas $MgSiO_3$ and Mg_2SiO_4 melt simulations at 3000 K yielded 12.5 mol% and 15 mol%, respectively.[101,132,133] Here, we report ab initio MD simulations on orthosilicate Na_4SiO_4. The orthosilicate composition was chosen because BO and O^{2-} disappear simultaneously from an orthosilicate glass or melt if Rxn. (1) goes to completion, yielding only NBO: at this composition the presence of either reactant, BO or O^{2-}, necessarily implies the presence of the other. No previous MD calculations have been performed on the Na_4SiO_4 composition.

Micro-canonical ensemble (constant-energy, constant-volume) first-principles molecular dynamics (MD) calculations were performed on Na_4SiO_4 and Mg_2SiO_4 using the Vienna *ab Initio* simulation package (VASP[134,135]). The core electrons of each atom were replaced by ultrasoft pseudopotentials.[136,137] The generalized gradient approximation[138] with the Perdew–Burke–Ernzerhof parametrization[139] was used for the exchange-correlation functional. The valence electron orbitals were expanded in a plane-wave basis set, and Brillouin zone sampling was performed at the Γ point. To verify the results, calculations were also performed on Na_4SiO_4 using the more accurate projector augmented-wave (PAW33) potential.[135] A 396 eV energy cutoff was used in all calculations.

Following de Koker *et al.*[101] and Tse,[134] the model systems consist of 16 formula units (Na_4SiO_4 = 144 atoms and Mg_2SiO_4 = 112 atoms). The melted glasses were obtained by heating crystalline Na_4SiO_4[140] to between 4000 K and 5000 K. Such heating is required to rapidly disorder the crystalline structure.[141] Our heating, cooling, and annealing protocol is similar to previous simulations on Mg-silicates.[132,133] The systems were melted and annealed for at least 3 ps at high temperature, then cooled for several ps per temperature step, with the final structure in all runs being annealed at 300 K for an additional 3 ps. The full heating and cooling cycle took over 20 ps.

In one run, Na_4SiO_4 was heated from 300 K to 4000 K, then cooled in steps to 3000 K, 2000 K, 1000 K, 500 K, and 300 K. In a second run, Na_4SiO_4 was heated from 300 K in steps to 3000 K, 4000 K, and 4500 K, then cooled in steps to 2500 K, 1000 K, and 300 K. A third run used the more accurate PAW33 potential. It melted at 4500 K and was then cooled to 4000 K, 2500 K, 1000 K, and 300 K. With this cooling rate (necessary for reasonable computational cost), it is not possible to guarantee that the resulting low-temperature structure is the true equilibrium glass structure rather than a frozen melt; nevertheless, we refer to it as a glass. The three runs yield similar Si–O bond lengths and O–Si–O angles, as well as similar numbers of BO atoms at 1000 K and 300 K, indicating that the results are not particularly sensitive to the pseudopotential used or the cooling rate.

Figures 13(a) and 13(b) show the silicate network in Na_4SiO_4 at 1000 K and 300 K, where Na atoms, Si atoms, and O atoms bonded to Si are shown to emphasize the abundance of bridging oxygen atoms present. The snapshots demonstrate that, upon heating, the structure becomes fully disordered, with no vestige of the original crystalline Na_4SiO_4 structure. Heating to 5000 K results in many dissociated Si–O bonds, producing SiO_4, SiO_3, SiO_2, and Si_2O_7 units; there is one BO in the system. Decreasing the temperature to 3000 K results in the loss of all SiO_2 units and all but one SiO_3 unit. One Si_2O_7 and one Si_3O_{10} unit are present, indicating three BO atoms. Below the melting point (1360 K), all Si atoms are coordinated to four O atoms, with three Si_2O_7 units (ringed) present at 1000 K (Fig. 13(a)) and two at 300 K (Fig. 13(b)), indicating 3 and 2 BO atoms respectively. One FO is evident in Fig. 13(b). The PAW potential run yielded 4 BO and 4 Si_2O_7 units at 300 K. These three Na-silicate simulations together provide results consistent with MD simulations using larger system sizes, as demonstrated by Van Ginhoven *et al.*[142]

It can be difficult to count the number of FO, as indicated by a reviewer concerned with Na–O and Si–O cutoff distances. One FO was identified at the top right of Fig. 13(b). For this orthosilicate glass, it is easier to estimate the FO content from the number of dimer Si_2O_7 groups using Eq. (4), because each dimer gives rise to one FO (Eq. (4))

$$2Q^0 \Leftrightarrow 2Q^1 + \mathrm{FO},$$

or

$$2\,SiO_4 \Leftrightarrow Si_2O_7 + \mathrm{FO}.$$

From this equilibrium equation, the number of dimers is equal to the number of FO (and, as an aside, the number of BO, one per dimer, is also equal to the number of FO). We observe between 2 and 4 dimers in our calculations, which yields an average of three FO — about 5% of the 64 O atoms in our 144-atom simulation.

The calculated Si–O bond lengths are within the range observed by Baur *et al.*[140] for crystalline Na_4SiO_4 (1.59–1.68 Å) and are similar to bond lengths obtained from neutron scattering, EXAFS, and MD calculations using empirical potentials for Na silicate glasses (1.61–1.67 Å[8–15]). Our two other Na_4SiO_4 simulations yield Si–O average bond lengths within 0.01 Å of the above values. The O–Si–O bond angles are also similar to those obtained for crystalline Na_4SiO_4 (103.10°–116.90°[140]). The simulated Na–O bond lengths (av. $= 2.305 \pm 0.108$ Å) are within the range observed for crystalline Na_4SiO_4 (2.28–2.55 Å[140]) and for Na silicate glasses (2.31–2.4 Å[11]).

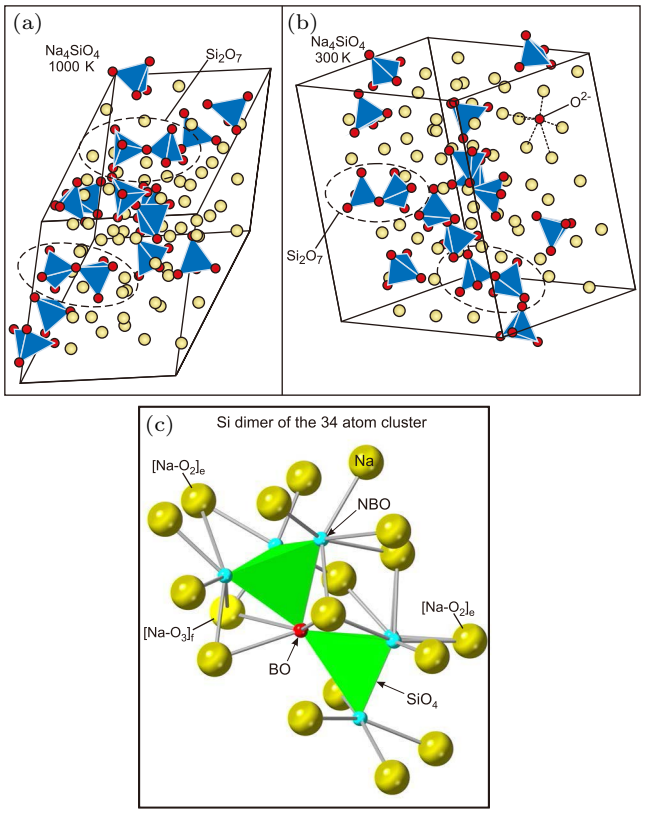


Fig. 13. Dimers and FO from the 144 atom and 324 atom[143] MD simulations. (a) Na_4SiO_4 at 1000 K; (b) Na_4SiO_4 at 300 K for the 144 atom simulation (O = red balls, Na = yellow balls, Si = blue atoms or SiO_n units); (c) a blowup of a dimer from the 324 atom simulation (NBO = blue balls; BO = red ball; Na = yellow balls; SiO_4 = green units). Note the two Si_2O_7 dimers (ringed) in both (a) and (b), and the O^{2-} (FO) in (b) at the top right.

In Figs. 13(a) and 13(b) there are two obvious Si_2O_7 dimers out of sixteen initial SiO_4 units. One other Si_2O_7 unit is less obvious. As previously noted, the FO content of the Na_4SiO_4 glass simulations averages about 5 mol% of total oxygen (3 out of 64). Its abundance is somewhat greater in simulated high-temperature Mg_2SiO_4 and $MgSiO_3$ melts.[45,101,103,132,133] The presence of FO indicates that Rxn. (1) does not go to completion in alkali or alkaline-earth silicate glasses, as discussed above.

Finally, we have performed a similar MD simulation on a larger 324-atom cluster of Na_4SiO_4.[143] This simulation also revealed a number of Si_2O_7 dimers with associated FO. A 34-atom cluster from this calculation shows the structure of one of these dimers in detail (Fig. 13(c)).

2.8. Other physical and chemical evidence for the importance of FO

There are many examples from the literature which show that FO is critically important for the physical and chemical properties of these glasses. Indeed, as mentioned in a previous paper,[69] FO should be treated as a master variable in silicate melts, just as H^+ (pH) is in aqueous solutions. Using both polymerization and disproportionation reactions at the atomic level,[144,145] we have shown that FO is directly involved in fundamental physical properties via nucleophilic substitution (S_N) reactions when Lewis bases such as FO and NBO attack SiO_4 tetrahedra to form five-coordinate Si^V. FO must be a stronger nucleophile than NBO or BO, and FO should be the dominant nucleophile in basic melts with $\leq$ 40–50 mol% SiO_2. Melting of crystalline alkali and alkaline-earth orthosilicates and metasilicates produces more polymerized melts than their precursor crystals, and FO is directly involved. We have shown, for example, that melting of crystalline Na_2SiO_3[55,99,144] results in conversion of Q^2 species of the crystal to Q^3 and FO. We have also shown that oxidation of Fe^{2+} to Fe^{3+} in mid-ocean ridge basaltic melts and glasses (MORBs) with mol% $SiO_2 \leq 50$ mol% is probably driven by FO present in all alkali and alkaline-earth melts. In addition, we show that S_N reactions involving FO are critical for other physical properties such as diffusion, conductivity, and viscosity.[145]

Regarding the effect of K on other physical properties, it is well known that replacement of Li, Na, or Mg by K can enhance the strength of glasses by 2–4 times, improve hardness, and decrease fragment size.[146,147] For example, the Raman spectrum of an initial 30 mol% Li_2O glass shows a strong Q^3 envelope along with a weaker Q^2 peak of about 15% of the total spectral intensity.[82,146] After ion exchange of Li for K, the Q^2 intensity decreases from $\sim$ 15% to about 9% of the total intensity (Fig. 6 in Ref. [146]). This shows that the K-rich surface is more polymerized than the Li bulk due to conversion of Q^2 to Q^3 via the polymerization reaction, which produces more FO. Such polymerization will increase the strength of the glass surface.

We briefly consider the importance of FO for the chemistry of silicate glasses. Stolper[33,34] initially showed from IR spectra that there were two species in his melts after reaction with both CO_2 and H_2O: CO_2 and CO_3^{2-}, and H_2O and OH^- respectively, and it was simple to write

$$CO_2(\text{molecular}) + O_r^{=} \Leftrightarrow CO_3^{2-}, \tag{20}$$

and

$$H_2O(\text{molecular}) + O_r^{=} \Leftrightarrow 2OH^-, \tag{21}$$

where O_r represents a reactive O species (BO, NBO, or FO). Stolper noticed that at low Na_2O glass compositions, mostly molecular CO_2 and H_2O were present after reaction with CO_2 and H_2O respectively; but for higher Na_2O mol% glasses, only CO_3^{2-} and OH^- were present. Both NBO and FO increase with Na_2O (Figs. 2 and 3), but FO increases much faster than NBO (Figs. 2 and 3), and FO is likely the reactive O species.[35]

The Raman and NMR communities did not accept the presence of FO in these glasses, and, through conventional wisdom, the community adopted the convention that NBO was the reactive O species. It is much more likely that FO

is the reactive species based on expected reactivity and steric effects.[35] In support, Eggler and Rosenhauer[148] in 1979 recognized that FO is the favorable species because the reaction "involves no rearrangement of the silicate network and will be strongly favored if such oxides are present". Also, there is good evidence for "free-ionic clusters" (FIC, with CO_3^{2-} bonded only to a cation) in low SiO_2 glasses reacted with CO_2.[149] FICs would be expected if FO is the reactive O species in Eq. (20).

There is also evidence that the reactivity of K glasses with gases such as H_2O and CO_2 is significantly enhanced compared with the reactivity of Na glasses of the same composition. For example, we have suggested[35] that FO is likely to have a large influence on the reactivity of K silicate glasses and may explain their exceptional reactivity with H_2O. Also, in relatively low-SiO_2 glasses with about 45 mol% SiO_2 (with 7 mol% Al_2O_3, 15 mol% (Mg,Ca)O and 20 mol% $(Na_x, K_{1-x})_2O$ ($x = 0$ to 1)), the uptake of CO_2 (as shown by the CO_3^{2-} IR band at 1070 cm^{-1}) is significantly enhanced when Na is replaced by K, as expected from the larger FO content in K glasses. For example, for glasses equilibrated at high pressure (50 MPa) and high temperature (1250 °C), the CO_2 solubility is $\sim$ 1.75 wt% in the K-free glass ($x = 1$) and increases to $\sim$ 3.0 wt% in the Na-free glass ($x = 0$).[150]

Finally, it seems appropriate to comment on the possible effect of FO on the bioactivity of soda-lime silicate glasses. Although commercial bioactive glasses contain several mol% P_2O_5, low-silica glasses with $\sim$ 50 mol% SiO_2 and no P_2O_5 have also been shown to promote *in vivo* bone formation or osteogenesis. Two recent ^{29}Si NMR and Raman studies on soda-lime silicate glasses with $\sim$ 70–50 mol% SiO_2, $\sim$ 15–25 mol% CaO, and $\sim$ 15–25 mol% Na_2O have attempted to correlate the observed Q species distributions with chemical reactivity.[77,78] For example, the ^{29}Si NMR spectrum of a metasilicate glass with 50 mol% SiO_2, 25 mol% CaO, and 25 mol% Na_2O shows a poorly resolved spectrum indicating a weak Q^1 peak (4.5%), a strong Q^2 peak (71.8%), and a moderate Q^3 peak (23.7%). Network connectivity (NC)[151,152] was used to discuss structural differences, and BO and NBO can be readily calculated from Eqs. (8) and (9). Note that $NC = BO/Si = 4 - (NBO/Si)$, where 4 is the number of Si–O bonds. As discussed above, $Q^3 \gg Q^1$ indicates polymerization and mol% FO (ignored in Ref. [77,78]). Calculation of FO using Eqs. (14) and (15) yields 2 mol% FO, as is also suggested by their higher-than-expected NC ($BO/Si = 2.19$ and $NBO/Si = 1.81$) versus the analyzed NC (BO) value of 2.09 ($NBO/Si = 1.91$). The decrease in NBO/T by 0.1 (1.91 to 1.81) also indicates $\sim$ 2 mol% FO, as noted earlier in this paper and in Table 1 of Ref. [145]. We suggest that this FO is the most reactive species in these glasses. Obviously, more research is needed to confirm this suggestion.

3. Conclusion

We have realized our most important objective. We have presented overwhelming evidence for mol% FO in Na and K glasses from all three spectroscopies (O 1s XPS, ^{29}Si NMR, and Raman), with 1.9 ($\pm$1) mol% in 40 mol% Na_2O glass and $\geq$ 7 mol% in 50 mol% K_2O glass. The evidence is too strong to ignore. The essential solid-solution equilibrium treatment (Eqs. (1)–(3)) shows that significant FO must also be present at much lower mol% M_2O. For example, for K_2O glasses, there should still be $\geq$ 1 mol% FO in K glasses with $\sim$ 30 mol% K_2O, as also demonstrated by our O 1s XPS results. MD simulations on Na_4SiO_4 are also consistent with substantial FO, showing $\sim$ 5 mol% FO in a Na_4SiO_4 glass. Also, the ^{29}Si NMR spectra of 50 mol% Rb_2O and Cs_2O silicates[67,68] also show FO contents comparable to K glasses. We conclude that alkali silicate glasses show comparable (or greater) FO% than alkaline-earth silicate glasses of comparable composition.

The justification of FO= 0 for alkali glasses using the thermodynamics of crystalline phases and the low crystal-field strengths of alkali cations is not appropriate. The ^{29}Si NMR spectra of the well-resolved 40 mol% Na_2O and 50 mol% K_2O glasses are critical to the present analysis; however, the poor resolution of nearly all other ^{29}Si NMR spectra of alkali and alkaline-earth silicate glasses makes it difficult to justify the use of ^{29}Si NMR alone to quantify Q species distributions in most silicate glasses.

After reassignment of the Raman spectra (using Lorentzian peak shapes and M–BO interactions which broaden and distort the Q^3 peak), we have shown that the Raman spectra and some ^{29}Si NMR spectra are semi-quantitatively consistent, as initially envisaged by Franz and Mysen[52] and McMillan.[110] For example, in both spectroscopies there is one resolved peak per Q species, there is a good correlation of peak positions for all Q species, and even the relative widths of the Q species peaks are similar. Most importantly, the Raman cross sections are close to unity, and a reasonable estimate of FO can be obtained from the raw Raman spectra. For $\gg$ 40 mol% samples, these spectra can now be fit, assigned, and quantified as well as other spectroscopies such as Mössbauer, XPS, or NMR.

We have also shown the importance of FO for determining physical and chemical properties such as melting and strength of glasses, reactions with gases such as H_2O and CO_2, and bioactivity. There is a need for more accurate measurements of FO (and more accurate Q species amounts and more accurate K_3 values), which should enable better predictions of these physical and chemical properties.

Following Richet's article on the development of scientific truth[60] in the earth sciences, there was a scientific "consensus" in the 1980s, 1990s, and 2000s that disproportionation alone was responsible for Q species distributions. This led

to rejection of papers that contradicted the accepted interpretation, along with "adjusting" results[51] to fit the prevailing model. There are some analogies with the controversy over the age of the Earth from the 1860s to the 1930s.[60] The geological community had a consensus from 1860–1905 that the age of the Earth was 20–100 M years. With the discovery of radioactivity in 1895, a new scientific community (physicists) using a new technique (isotopic dating) was rejected for decades by the geological community, which had to "adjust" their results. Richet concludes that "if truth can only be approached little by little, the intrusion of outsiders into the debate is certainly not to be rejected but rather encouraged to break with any group thinking".

Acknowledgments

We are very pleased to help celebrate the many outstanding research accomplishments (in many scientific disciplines) of our colleague John Tse over the last 50 years, including close to 50 joint publications and his calculations in this paper. We thank our respective departments and universities for logistical support required to conduct this study. JST acknowledges computational facilities provided by the Argonne Leadership Computing Facility (ALCF) and the Fugaku computer system at RIKEN, Japan. We also thank the solid-state NMR spectroscopists, Profs. H. Eckert and Y. Huang, for their confirmation that higher magnetic fields do not improve the ^{29}Si resolution of silicate glasses.

References

[1] Pant A K and Cruikshank D W J 1968 *Acta Cryst. B* **24** 13
[2] McDonald W S and Cruikshank D W J 1967 *Acta Cryst. B* **22** 37
[3] Smythe J R 1974 *Amer. Mineral.* **59** 345
[4] Birle J D, Gibbs G V, Moore P B and Smith J V 1968 *Amer. Mineral.* **53** 807
[5] Zachariasen W H 1932 *J. Am. Chem. Soc.* **54** 3841
[6] Warren B E 1934 *Phys. Rev.* **45** 657
[7] Warren B E and Biscoe J 1938 *J. Am. Ceram. Soc.* **21** 259
[8] Greaves G N, Fontaine A, Lagarde P, Raoux D and Gurman S J 1981 *Nature* **293** 611
[9] Henderson G S 1995 *J. Non-Cryst. Sol.* **183** 43
[10] Hannon A C, Vaishnav S, Alderman O L G and Bingham P A 2021 *J. Amer. Ceram. Soc.* **104** 6155
[11] Du J and Cormack A N 2004 *J. Non-Cryst. Sol.* **349** 66
[12] Mountjoy G 2007 *J. Non-Cryst. Sol.* **353** 1849
[13] Cormack A N, Du J and Zeitler T R 2003 *J. Non-Cryst. Sol.* **323** 147
[14] Tilocca A 2010 *J. Chem. Phys.* **133** 014701
[15] Kilymis D, Ispas S, Hehlen B, Peuget S and Delaye J M 2019 *Phys. Rev. B* **99** 054209
[16] Mysen B O and Richet P 2019 *Silicate Glasses and Melts, Properties and Structure*, 2nd edition (Amsterdam: Elsevier)
[17] Henderson G S 2005 *Canadian Mineral.* **43** 1921
[18] Moulton B J A and Henderson G S 2021 *Encycl. Mater.: Tech. Ceram. Glasses* **2** 462
[19] Greaves G N 1985 *J. Non-Cryst. Sol.* **71** 203
[20] Nesbitt H W, Henderson G S, Bancroft G M and Ho R 2015 *J. Non-Cryst. Sol.* **409** 139
[21] Nesbitt H W, Henderson G S, Bancroft G M, Sawyer R and Secco R A 2017 *Chem. Geol.* **461** 13
[22] Fincham C F B and Richardson F D 1954 *Proceed. Royal Soc. London A* **223** 40
[23] Brawer S A and White W B 1975 *J. Chem. Phys.* **63** 2421
[24] Virgo D, Mysen B O and Kushiro I 1980 *Science* **208** 1371
[25] Furukawa T, Fox K and White W B 1981 *J. Chem. Phys.* **75** 3226
[26] Mysen B O, Finger L W, Virgo D and Seifert F A 1982 *Amer. Min.* **67** 686
[27] Matson D W, Sharma S K and Philpotts J A 1983 *J. Non-Cryst. Solids* **58** 323
[28] McMillan P F 1984 *Amer. Mineral.* **69** 622
[29] Schramm C M, de Jong B H W S and Parziale V E 1985 *J. Am. Chem. Soc.* **106** 4396
[30] Selvaray U, Rao K J, Rao C N R and Thomas J M 1985 *Chem Phys Lett* **114** 24
[31] Murdoch J B, Stebbins J F and Carmichael I S E 1985 *Amer. Min.* **70** 332
[32] Stebbins J F 1987 *Nature* **330** 465
[33] Fine G and Stolper E 1985 *Contrib. Mineral. Petrol.* **91** 105
[34] Stolper E 1982 *Contrib. Mineral. Petrol.* **81** 1
[35] Sawyer R, Nesbitt H W, Bancroft G M, Thibault Y and Secco R A 2015 *Can. J. Chem.* **93** 60
[36] Bruckner R, Chun H-U, Goretzki H and Sammet 1980 *J. Non-Cryst. Solids* **42** 49
[37] Veal B W, Lam D J and Paulikas A P 1982 *J. Non-Cryst. Solids* **49** 309
[38] Toop G W and Samis C S 1962 *Trans. Metall. Soc. AIME* **224** 878
[39] Pearce M L 1964 *J. Amer. Ceram. Soc.* **47** 342
[40] Hess P C 1971 *Geochim. Cosmochim. Acta* **35** 289
[41] Maekawa H, Maekawa T, Kawamura K and Yokokawa T 1991 *J. Non-Cryst. Solids* **127** 53
[42] Zhang P, Dunlap C, Florian F, Grandinetti P J, Farnan I and Stebbins J F 1996 *J. Non-Cryst. Solids* **204** 294
[43] Shaller T, Stebbins J F and Wilding M C 1999 *J. Non-Cryst. Solids* **243** 146
[44] Olivier L, Yuan X, Cormack A N and Jager C 2001 *J. Non-Cryst. Solids* **293-295** 53
[45] Davis M C, Kaseman D C, Parvani S M, Sanders K J, Grandinetti P J, Massiot D and Florian P 2010 *J. Phys. Chem. A* **114** 5503
[46] Malfait W J, Halter W E, Morizet Y, Meier B H and Verel R 2007 *Geochim. Cosmochim. Acta* **71** 6002
[47] Schaller T, Stebbins J F and Wilder M C 1999 *J. Non-Cryst. Solids* **243** 146
[48] Sen S and Youngman R E 2003 *J. Non-Cryst. Solids* **331** 100
[49] McMillan P F, Wolf G H and Poe B T 1992 *Chem. Geol.* **96** 351
[50] McMillan P F and Wolf G H 1995 *Rev. Min. Geochem.* **32** 247
[51] Mysen B O and Frantz J D 1992 *Chem. Geol.* **96** 321
[52] Frantz J D and Mysen B O 1995 *Chem. Geol.* **121** 155
[53] Mysen B O and Frantz J D 1993 *Euro. J. Mineral.* **5** 393
[54] Mysen B O and Frantz J D 1994 *Contrib. Min. Petrol.* **117** 1
[55] Richet P, Mysen B O and Andrault D 1996 *Chem. Mineral.* **23** 157
[56] You J L, Jiang G C and Xu K D 2001 *J. Non-Cryst. Solids* **282** 125
[57] Neuville D R 2006 *Chem. Geol.* **229** 28
[58] Malfait W J, Zakaznova-Herzog V P and Halter W E 2007 *J. Non-Cryst. Solids* **353** 4029
[59] Malfait W J, Zakaznova-Herzog V P and Halter W E 2008 *Amer. Min.* **93** 1505
[60] Richet P 2025 *Atti Docum. Accad. Naz. Sci.* **70** 227
[61] Stebbins J F and Sen S 2013 *J. Non-Cryst. Solids* **368** 17
[62] Stebbins J F 2017 *Chem. Geol.* **461** 2
[63] Stebbins J F 2020 *J. Non-Cryst. Solids X* **6** 100049
[64] Nesbitt H W, Bancroft G M, Henderson G S, Ho R, Dalby K N, Huang Y and Yan Z 2011 *J. Non-Cryst. Solids* **357** 170
[65] Dalby K N, Nesbitt H W, Zakaznova-Herzog V P and King P L 2007 *Geochim. Cosmochim Acta* **71** 4297
[66] Fayon F, Bessada C, Massiot D M, Farnan I and Coutures J P 1998 *J. Non-Cryst. Solids* **232-234** 403
[67] Malfait W J 2015 *Can. J. Chem* **93** 578
[68] Nesbitt H W, Bancroft G M, Thibault Y, Sawyer R and Secco R A 2015 *Can. J. Chem* **93** 581
[69] Nesbitt H W, Bancroft G M, Henderson G S, Sawyer R and Secco R A 2015 *Amer. Min.* **100** 2566
[70] Kalampounias A G, Nasikas N K and Papatheodorou G N 2009 *J. Chem. Phys.* **131** 114513
[71] Nasikas N K, Edwards T G, Sen S and Papatheodorou G N 2012 *J. Phys. Chem. B* **116** 2696

[72] Nasikas N K, Chrissanthopoulos A, Bouropoulos N, Sen S and Papatheodorou G N 2011 *Chem. Mater.* **23** 3692
[73] Retsinas A, Kalampounias A G and Papatheodorou G N 2014 *J. Non-Cryst. Solids* **383** 38
[74] LeLosq C and Neuville D R 2017 *J. Non-Cryst. Solids* **463** 175
[75] Cicconi M R, de Ligny D, Veber A, Neuville D R and Baudelet F 2021 *J. Non-Cryst. Solids* **563** 120785
[76] Koroleva O N, Shtenberg M V and Osipov A 2023 *Minerals* **13** 94
[77] Jin Z R, Neuville D R and Brauer D S 2025 *RSC Advances* **15** 4997
[78] Jin Z R, Neuville D, Chartier C, Kachanov P, Kroeker S, Gin S, Du J and Brauer D S 2025 *J. Material. Chem.* **13** 3448
[79] O'Shaughnessy C, Henderson G S, Nesbitt H W, Bancroft G M and Neuville D R 2017 *Chem. Geol.* **461** 82
[80] Nesbitt H W, O'Shaughnessy C, Henderson G S, Bancroft G M and Neuville D R 2018 *Chem. Geol.* **505** 1
[81] Bancroft G M, Nesbitt H W, Henderson G S, O-Shaughnessy C, Withers A C and Neuville D R 2018 *J. Non-Cryst. Solids* **484** 72
[82] O'Shaughnessy C, Henderson G S, Nesbitt H W, Bancroft G M and Neuville D R 2020 *J. Am. Ceram. Soc.* **103** 3991
[83] Nesbitt H W, Henderson G S, Bancroft G M and Neuville D R 2021 *Chem. Geol.* **562** 120040
[84] Moulton B J A, Silva L D, Doerenkamp C, Lozano H, Zanotto E D, Eckert H and Pizani P S 2021 *Chem. Geol.* **586** 120611
[85] Moulton B J A, Picinin A, Silva L D, Doerenkamp C, Lozano H, Sampaio D, Zanotto E D, Du J, Eckert H and Pizani P S 2022 *J. Non-Cryst. Solids* **583** 121477
[86] Walsh C, Schroeder A, Vaishnav S, Barrow N, Packard M J, Hannon A C, Feller S and Bingham P A 2026 submitted
[87] Sawyer R, Nesbitt H W and Secco R A 2012 *J Non-Cryst. Solids* **358** 290
[88] Lee S K and Kim E J 2015 *J. Phys. Chem. C* **119** 748
[89] Neuville D R, DeLigny D and Henderson G S 2014 *Rev. Mineral. Geochem.* **78** 509
[90] Sen S, Stebbins J F, Kroeker S, Hung I and Gan Z 2023 *J. Phys. Chem B* **127** 10659
[91] Hochella M F 1988 *Rev. Mineral. Geochem.* **18** 573
[92] Bancroft G M and Nesbitt H W 2014 *Rev. Mineral. Geochem.* **78** 271
[93] Pintori G and Cattaruzza E 2022 *Opt. Mater.* **13** 100108
[94] Grey LH, Nie H Y and Biesinger M C 2024 *Appl. Surf. Sci.* **653** 159319
[95] Nesbitt H W, Bancroft G M, Davidson R, McIntyre N S and Pratt A R 2004 *Amer. Mineral.* **89** 878
[96] Bancroft G M, Nesbitt H W, Ho R, Shaw D M, Tse J S and Biesinger M C 2009 *Phys. Rev. B* **80** 075405
[97] Bancroft G M 1973 *Mössbauer Spectroscopy: An Introduction for Inorganic Chemists and Geochemists* (London:McGraw-Hill)
[98] Sen S and Youngman R E 2003 *J. Non-Cryst. Solids* **331** 100
[99] Zhang P, Grandinetti P J and Stebbins J F 1997 *J. Phys. Chem. B* **101** 4004
[100] Nesbitt H W, Henderson G S and Bancroft G M 2020 *Amer. Min.* **105** 716
[101] de Koker N P, Stixrude L and Karki B B 2009 *Geochim. Cosmochim. Acta* **72** 1427
[102] Al-Hasni B M and Mountjoy G 2014 *J. Non-Cryst. Solids* **400** 33
[103] Sen S and Tangeman J 2008 *Amer. Min.* **93** 946
[104] Thompson L M, McCarty R J and Stebbins J F 2012 *J. Non-Cryst. Solids* **358** 2999
[105] Matsumoto S, Nanba T and Miura Y 1998 *J. Ceramic Soc. Japan* **106** 415
[106] Huheey J E 1978 *Inorganic Chemistry: Principles of Structure and Reactivity* 2nd edition (New York: Harper International)
[107] Ching W Y, Murray R A, Lam D J and Veal B W 1983 *Phys. Rev. B* **28** 4724
[108] de Jong B H W S, Super H T J, Spek A L, Veldman N, Nachtegaal G and Fischer J C 1998 *Acta Cryst.* **54** 568
[109] Greaves G N, Smith W, Giulotto E and Pantos E 1997 *J. Non-Cryst. Sol.* **222** 13
[110] McMillan P F, Wolf G H and Poe B T 1992 *Chem. Geol.* **96** 351
[111] Bancroft G M, Dean P A W, Henderson G S and Nesbiott H W 2023 *AIP Advances* **13** 125216
[112] Haken H and Wolf H C 1996 *The Physics of Atoms and Quanta* (5th edition) (Berlin: Springer Verlag) pp. 292
[113] Efimov A M 1996 *J. Non-Cryst. Solids* **253** 95
[114] Nesbitt H W, Bancroft G M and Henderson G S 2018 *Amer. Min.* **103** 966
[115] Nesbitt H W, Bancroft G M, Henderson G S, Richet P and O'Shaughnessy 2017 *Amer. Min.* **102** 412
[116] Rossano S and Mysen B 2012 *Eur. Mineral. Union Notes in Mineralogy* **12** 321
[117] Kamitsos E and Risen W M 1984 *J. Non-Cryst. Solids* **65** 333
[118] Umesaki N, Takahashi M, Tasumisago M and Minami T 1993 *J. Mat. Sci.* **28** 3473
[119] Zotov N, Ebbsji I, Timpel D and Keppler H 1999 *Phys. Rev. B* **60** 6383
[120] Henderson G S, Bancroft G M, Nesbitt H W, Dean P A W and Cicconi M R 2025 *Phys. Chem. Glasses - Euro. J. Glass Sci. Technol Part B* **66** 63
[121] Nesbitt H W, Dean P A W, Bancroft G M and Henderson G S 2022 *Amer. Min.* **107** 2044
[122] Nesbitt H W, Henderson G S, Bancroft G M and O'Shaughnessy C 2017 *Chem. Geol.* **461** 65
[123] You J L, Jiang G C, Hou H Y, Wu Y Q and Xu K D 2005 *J. Raman Spectros.* **36** 237
[124] Pannefieu S, Le Losq C, Florian P and Moretti R J 2024 *J. Non-Cryst. Solids* **637** 123056
[125] Fraser D G 1977 *Thermodynamics in Geology*, (ed. D G Fraser) D Reidel Pub. Co. Dordrecht, p. 301
[126] Fraser D G 2005 *Ann. Geophys.* **48** 549
[127] Koroleva O N, Anfilogov V N, Shatsky A and Litasov K D 2013 *J. Non-Cryst. Solids* **375** 62
[128] Tossell J A 1984 *Phys. Chem. Mineral* **10** 137
[129] Nesbitt H W, Bancroft G M and Ho R 2017 *Surf. Interface Anal.* **49** 1298
[130] Nesbitt H W, Bancroft G M, Sawyer R, Secco R A and Henderson G S 2024 *J. Non-Cryst. Solids* **637** 123044
[131] LeLosq C and Neuville D R 2017 *J. Non-Cryst. Solids* **463** 175
[132] Karki B 2010 *Rev. Mineral. Geochem.* **71** 355
[133] Karki B, Bhattarai D, Mookherjee M and Stixrude L 2010 *Phys. Chem. Miner.* **37** 103
[134] Tse J S 2002 *Annu. Rev. Phys. Chem.* **53** 249
[135] Kresse G and Furthmüller J 1996 *Comput. Mat. Sci.* **6** 15
[136] Kresse G and Joubert J 1999 *Phys. Rev.B* **59** 1758
[137] Vanderbilt D 1990 *Phys. Rev. B* **41** 7892
[138] Langreth D C and Perdew J P 1980 *Phys. Rev.B* **21** 5469
[139] Perdew J P, Burke K and Ernzerhof M 1996 *Phys. Rev. Lett.* **77** 3865
[140] Baur W H, Halwax E and Vollenkle H 1986 *Monatsh. Chem.* **117** 793
[141] Phillpot S R, Yip S and Wolfe D 1989 *Comput. Phys.* **3** 20
[142] Van Ginhoven R M, Jonsson H and Corrales L R 2005 *Phys. Rev. B* **71** 024208
[143] Nesbitt H W, Henderson G S, Dean P A W, Tse J S, Kuang H and Bancroft G M 2026 *Phys. Chem. Glasses* (submitted)
[144] Nesbitt H W, Bancroft G M, Henderson G S, Richet P and O'Shaughnessy C 2017 *Amer. Min.* **102** 412
[145] Nesbitt H W, Bancroft G M and Henderson G S 2020 *Chem. Geol.* **555** 119818
[146] Calahoo C, Zwanziger J W and Butler I S 2016 *J. Phys. Chem.* **120** 7213
[147] Kumar S, Kumar D and Singh K 2023 *J. Phys. Chem. Sol.* **181** 111523
[148] Eggler D H and Rosenhauer M 1978 *Amer. J. Sci.* **278** 64
[149] Morizet Y, Florian P, Paris M and Gaillard F 2017 *Amer. Min.* **102** 1561
[150] Morizet Y, Paris M, Gaillard F and Scaillet B 2014 *Geochim. et Cosmochim. Acta* **141** 45
[151] Hupa L 2018 In *Bioactive Glasses: Materials, Properties and Applications*, Chapter 1, pp. 1 (Elsevier)
[152] Hill R G and Brauer D S 2011 *J. Non-Cryst. Solids* **357** 3884